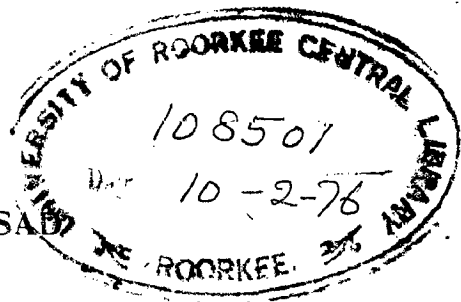# HEAT TRANSFER STUDIES ON A THERMOSIPHON REBOILER

A THESIS
SUBMITTED IN PARTIAL FULFILMENT OF THE
REQUIREMENTS FOR THE AWARD OF THE DEGREE
OF
MASTER OF ENGINEERING
IN
CHEMICAL ENGINEERING
(EQUIPMENT AND PLANT DESIGN)

BY
RAMESHWAR PRASAD

DEPARTMENT OF CHEMICAL ENGINEERING
UNIVERSITY OF ROORKEE
ROORKEE (INDIA)
AUGUST, 1975

C E R T I F I C A T E

Certified that the thesis entitled "Heat Transfer Studies on a Thermosiphon Reboiler" which is being submitted by Sri Rameshwar Prasad in partial fulfilment of the requirements for the award of the degree of MASTER OF ENGINEERING IN CHEMICAL ENGINEERING (Plant and Equipment Design) at the University of Roorkee, is a record of candidate's own work carried out by him under the supervision and guidance of the undersigned. The matter embodied in this thesis has not been submitted for award of any other degree.

This is further certified that the candidate has worked for a period of about seven months for preparing this thesis at this University.

Roorkee
August 12 , 1975.

(S.S.Alam)
Reader
Chemical Engineering Department
University of Roorkee, Roorkee.

A C K N O W L E D G M E N T

A B S T R A C T

Experimental investigation of heat transfer to boiling of water and water-glycerine mixtures was carried out in a natural circulation single tube reboiler. The heat transfer section was an externally heated copper tube of 19.05 mm inside diameter and 940 mm long. The heating element, made of nichrome wire, was uniformly wound on the tube with porcelain beads as electrical insulator. The energy input to the test section was measured by wattmeters. Ten copper-constantan thermocouples were fixed on the tube wall along the length at intervals of 100 mm starting from the tube inlet to measure the wall temperatures. The liquid temperatures at inlet, exit and along the length were measured by copper constantan thermocouple probes. Different inlet liquid subcoolings in the range of $4^\circ C$ to $40^\circ C$ were used to get varying lengths in tube having single phase natural convection, subcooled boiling and bulk boiling regions of heat transfer. Heat flux values ranged from 10.66×10^3 to 24.88×10^3 W/m^2.

The local values of heat transfer coefficient in single phase convective region were found to remain almost unchanged along the tube length measured from the inlet but they increase sharply in subcooled boiling region, under identical conditions of inlet liquid subcooling and heat flux. The curves were found to shift to higher values of

heat transfer coefficient when either the inlet liquid subcooling was decreased or the heat flux was raised.

The heat transfer coefficients for water and water-glycerine mixtures in single phase natural convection were correlated by the following equation with a maximum error of $\pm$ 20 per cent.

$$Nu = 3.33 \times 10^{-3} (Gr \ Pr)^{0.44} (z_s/d)^{0.5} \qquad (4.2)$$

The equation is applicable for Gr Pr ranging from 7.11×10^6 to 19.0×10^6.

The experimental data on subcooled and saturated boiling of water and water-glycerine mixtures were found to be represented by a correlation in the following form

$$\frac{h_B}{h_c} = C_3 \left(\frac{\rho_L}{\rho_v} \cdot \frac{C}{\lambda} \cdot \frac{d}{z_s} \cdot \Delta t_{sub} \right)^{n_3} \left(\frac{t_L}{t_W} \cdot \frac{z}{d} \right)^m$$

$$(4.7)$$

The values of C_3, n_3 and m were 1.62×10^{-3}, -0.33 and 2 respectively for water and are given in Table 4.2 for water-glycerine mixtures. A maximum error of $\pm$ 40 per cent covered almost all the data points.

C O N T E N T S

Contents (Contd..)

LIST OF FIGURES

LIST OF TABLES

NOMENCLATURE

A	Surface area	m^2
C	Specific heat	kcal/kg $^\circ$C
d	Inside diameter of tube	m
D	Mass diffusivity	m^2/hr
g	Acceleration due to gravity	m/hr^2
G	Mass velocity	kg/m^2 hr
h	Heat transfer coefficient	kcal/hr m^2 $^\circ$C
i.d.	Inside diameter	m
o.d.	Outside diameter	m
k	Thermal conductivity	kcal/m.hr.$^\circ$C
mV	Millivolt	
q	Heat flux	W/m^2
Q	Heat input	W
t	Temperature	$^\circ$C
T	Absolute temperature	$^\circ$K
Δt	Temperature difference ($t_W - t_L$)	$^\circ$C
ΔT	Temperature drop across the liquid film	$^\circ$C
Δt_{sub}	Degree of subcooling at inlet	$^\circ$C
Δt_{sup}	Degree of superheat	$^\circ$C
U	Overall heat transfer coefficient	kcal/hr m^2 $^\circ$C
v	Velocity	m/hr
x	Two - phase mixture quality, weight fraction of total flow	
z	Distance along the test section from the bottom	m
z_s	Distance along the test section corresponding to the point of saturated boiling	m

GREEK LETTERS

α	Thermal diffusivity	m^2/hr
β	Thermal expansion coefficient	/$^\circ$C
λ	Latent heat of vaporisation	kcal/kg
μ	Viscosity	kg/m.hr
ρ	Density	kg/m^3
σ	Surface tension	m/hr

| v | Kinematic viscosity | | m^2/hr |
| ø | Volume fraction | | |

SUBSCRIPTS

atm	Atmosphere	out	Outlet
av	Average	Pred	Predicted
B	Boiling	s	Saturated
c	Convective	T	Total
Exptl	Experimental	TP	Two-Phase
H_2O	Water	V	Vapor
in	Inlet	W	Wall
L	Liquid	z	Distance
mix	Mixture		

DIMENSIONLESS GROUPS

Gr	Grashof number	$= \dfrac{gd^3 \beta \Delta t}{v^2}$
Nu	Nusselt number	$= \dfrac{hd}{k}$
Pr	Prandtl number	$= \dfrac{C\mu}{k}$
Re	Reynolds number	$= \dfrac{dv\rho}{\mu}$
X_{tt}	Lockhart-Martinellii parameter	$= \left(\dfrac{1-x}{x}\right)^{0.9} \left(\dfrac{\rho_V}{\rho_L}\right)^{0.5} \left(\dfrac{\mu_L}{\mu_V}\right)^{0.1}$

C H A P T E R   1

I N T R O D U C T I O N

Thermosiphon reboilers find wide applications in chemical and petrochemical industries mainly due to their mechanical simplicity and operation in the nucleate boiling regimes with attractively high heat fluxes. The vertical thermosiphons are generally hung on the tower , thus minimising foundation, structural, and plot area requirements. The discharge lines are directly connected to the tower with a minimum vapor pressure drop and vapor line costs. In evaporator services, the resistance to some types of fouling and ease of cleaning when fouled, make it a preferred unit.

The thermosiphon reboilers and natural circulation evaporator units essentially consist of a U-tube type system with movement due to density differences in the hot and cold legs of circulating system. The hot leg in these units is a one pass heat exchanger with process fluid to be vaporized in the vertical tubes. The predictions of flow and heat transfer rates are the two main requirements for the design of these equipments. Hydrodynamics and heat transfer phenomena in natural circulation boiling of liquids in vertical tubes are complicated owing to the presence of two phases (liquid and vapor) . Several steady

and   fluctuating flow modes are manifested during   heat
transfer to flowing two-phase boiling liquid-vapor mixture
as in a thermosiphon reboiler, depending upon the inlet
liquid temperature, heat flux, physical properties   of
flow components, tube geometry and orientation. The
various flow patterns exert different effects on the
hydrodynamic conditions near the heated wall and thus
they produce different frictional pressure drops and
different modes of heat transfer. This complicates the
investigation of a process, on the basis of sound theore-
tical considerations of heat and momentum transfer, to
any great accuracy . A fair amount of empiricism, there-
fore, becomes unavoidable in the studies on thermosiphon
reboilers.

During the last two decades, a number of experi-
mental studies have been conducted to investigate the
hydrodynamics and heat transfer aspects of natural cir-
culation boiling of liquids in vertical tubes. Based
on their data, some of the investigators have proposed
empirical correlations for computing pressure drop and
heat transfer coefficients. Most of these correlations
are in the modified forms of the equations for two phase
convective heat transfer based on the Lockhart-Martinelli
parameter. The nucleate boiling contributions are
accounted for through various correction factors using
film temperature difference as the main operating variable

and surface tension as the main transport property. Since the hydrodynamics of flow in boiling channel is governed by channel geometry, the applicability of each of these equations is restricted to particular geometry. Further the flow fluctuations inherent in natural circulation loops, modify the nucleating and convective contributions of boiling heat transfer and, as such, there is no method of accounting reliably for this influence. Almost all the studies on heat transfer aspect have been conducted using saturated liquids at the tube inlet and thus no work seems to have been published on subcooled boiling of liquids with natural convection in vertical tubes.

The present investigation was, therefore, undertaken with the following objectives :

1.   To obtain the wall and liquid temperature distri-
      butions along the tube length during natural circula-
      tion boiling of water and water-glycerine mixtures
      in a vertical tube at various wall heat fluxes and
      inlet liquid subcooling. From this information the
      local values of heat transfer coefficient may be com-
      puted.

2.   To develop, from experimental results, a correla-
      tion for predicting heat transfer coefficient in
      the single phase natural convection in a vertical
      tube.

3.   To obtain, based on experimental data, a general correlation for calculating the heat transfer coefficient during subcooled and saturated boiling of water and water-glycerine mixtures in a vertical tube under the conditions of natural circulation.

--

C H A P T E R   2

REVIEW   OF   LITERATURE

Boiling with natural   circulation in vertical tubes, as encountered in thermosiphon reboilers and natural circulation evaporators, has received the attention of many research workers from time to time. Hydrodynamics and heat transfer are the two major aspects of thermosiphon boiling systems which have been investigated with a view to provide reliable methods of designing them on industrial scale. The studies conducted on heat transfer are mostly experimental in nature and have resulted in a number of empirical and semi-empirical correlations. A brief review of these investigations is presented here.

Piret and Isbin [1] investigated six fluids : water, carbon tetrachloride, isopropyl and butyl alcohols, 35 wt.% K_2CO_3 and 50 wt. % K_2CO_3 at atmospheric pressure in a 1-in. nominal copper tube with 46.5 in. heated length. They used a modified Dittus Boelter equation to correlate the inside heat transfer coefficient. The equation is

$$\frac{h_{av}d}{k_L} = 0.0086 \left[\frac{dv_m\rho_L}{\mu_L}\right]^{0.8} \left[\frac{c_L\,\mu_L}{k_L}\right]^{0.6} \left[\frac{\sigma_{H_2O}}{\sigma_L}\right]^{0.33}$$

$$(2.1)$$

where v_m is a log mean velocity assuming a homogeneous flow and is given as

$$\left(v_{mix.out} - v_{L\ in}\right) \bigg/ \ln \left[v_{mix.out} \bigg/ v_{L\ in}\right]$$

Guerrieri and Talty [2] studied heat transfer to boiling of cyclohexane, methyl alcohol, benzene, pentane, and heptane in two single-tube natural-circulation vertical boilers which were light oil-heated brass tubes 0.75-in. i.d. by 6-ft long and 1-in. i.d. by 6.5-ft long respectively. Inside wall and boiling liquid temperatures were measured at 6-in. intervals along the tubes. Point heat transfer coefficient and the amount of vapour generated in each 6-in. section were calculated. Heat flux ranged from 2170 to 17,400 Btu/hr.ft^2; vapour at the tube outlet from 2.8 to 11.6 wt.% ; boiling film coefficient from 224 to 1172 Btu/hr.ft^2 $^\circ$F ; boiling film temperature drop from 6.1°F to 24.2 $^\circ$F. The transfer of heat in the tube boilers occurred simultaneously by convection and by nucleate boiling. The authors presented an analysis which accounts for both processes and based on this analysis, correlated their heat transfer results as ratio of the local two-phase convective heat transfer coefficient to the liquid-phase coefficient as a function of the reciprocal Lockhart-Martinelli parameter.

$$\frac{h_{TP}}{h_L} = 3.4 \left(\frac{1}{X_{tt}}\right)^{0.45} \qquad\qquad (2.2)$$

where h_L is the coefficient calculated from Dittus-Boelter equation for the liquid flowing alone.

$$h_L = 0.023 \left(\frac{k_L}{d}\right) \left(\frac{dG_T(1-x)}{\mu_L}\right)^{0.8} \left(\frac{c_L \ \mu_L}{k_L}\right)^{0.4} \qquad (2.3)$$

Dengler and Addoms [3] investigated the mechanism of boiling and heat transfer during vaporication of water in a vertical copper tube 1-in. i.d. by 20-ft long. The principal conclusions drawn are as follows :

(1) The mechanism of heat transfer during vaporisation in tubes is primarily convective. Nucleate boiling is dominant only under conditions of low liquid velocity and is gradually suppressed by the effect of vapour-induced forced flow.

(2) Operating variables exert independent and often opposing effects on each of the mechanisms:

(i) Increase in pressure may increase the heat transfer coefficient by its effect on nucleate boiling or decrease them in the range of two-phase convection by raising the average fluid density and thereby lowering the velocity.

(ii) Increase in temperature difference promotes nucleate boiling but has no direct effect on the convective coefficients.

(iii) Increase in total mass throughput increases the convective heat transfer but decreases the nucleate boiling heat transfer by lowering the available effective temperature driving force for nucleation.

They arrived at a correlation similar to that of Guerrieri and Talty

$$\frac{h_{TP}}{h_L} = 3.5 \left(\frac{1}{X_{tt}}\right)^{0.5} \tag{2.4}$$

where h_L is the coefficient calculated from Dittus-Boelter equation for the total flow.

$$h_L = 0.023 \left(\frac{k_L}{d}\right) \left(\frac{dG_T}{\mu_L}\right)^{0.8} \left(\frac{c_L \mu_L}{k_L}\right)^{0.4} \tag{2.5}$$

Lee et al [4] used a reboiler consisting of seven tubes in a bundle. The tubes were 1-in. o.d., 14 gauge, 10- ft long admiralty metal. They investigated seven liquids and presented data for a pressure range of 2 to 120 psia. Overall coefficients are presented as functions of overall temperature differences. The average inside-film coefficient and the maximum flux are presented in terms of dimensionless groups. The maximum flux was found for each fluid and system pressure. For heat fluxes above the maximum vapour-lock occurred. Recommendations include a maximum overall coefficient of 500 Btu/ hr. ft^2 $^{\circ}F$, and the need for giving particular attention to reboiler entrance and exit piping.

Johnson [5] measured circulation rates and overall temperature driving forces for a 15-in. shell reboiler containing 96 1-in., 12 gauge, 8-ft long tubes. One tube was equipped with a temperature probe to obtain local boiling stream temperatures. The systems investigated were water and a hydrocarbon having a normal boiling point of $80.8^{o}C$. Circulation rates were estimated by Kern's method . The Lockhart-Martinelli parameter is used to calculate friction and expansion losses for the two phase zone. Overall coefficients, driving forces fluxed, flow, and vapourisation rates are tabulated. Typical temperature profiles are shown for six runs on the hydrocarbon.

Ladiev [6] carried out experiments in three tubes 1500 mm long and 24, 28 and 52 mm diameter. Special attention was given to maintain identical conditions in all tubes. Heat transfer experimental results were correlated graphically for water at atmospheric pressure. The apparent liquid level in the tube had a significant effect on heat transfer for a given tube diameter. The rate of heat transfer decreased with an increase in the level. The sharp reduction in heat transfer at boiling in vertical tubes with inherent circulation was associated with inadequate flow in the upper part of the tube. Increase in tube diameter had no significant effec t on heat transfer rate, but circulation velocity decreased. Under vacuum, the general character of heat transfer was retained but its

absolute level was lower than that at atmospheric pressure.

Claire [7] obtained fundamental information regard-
ing heat transfer in a pilot evaporation plant. The coeffi-
cients of heat transfer for brass tubes and stainless steel
tubes of different lengths (6-ft and 4-ft) and 2.0 in.and
1.5 in.o.d. are compared. Tests with water boiling at
atmospheric pressure indicated that the heat transfer
was at maximum when the level of water was maintained at
about 1/3 of the tube height. For clean tubes the value
of U is always higher for brass tubes than for stainless
tubes.

Bergles et.al. [8] carried out experiments
on water at low pressures (below 100 psia) to investigate
the effec ts of tube length, inlet temperature, tube dia-
meter,and pressure on the critical heat flux. The results
were related to the instabilities of the slug-flow regime.
Critical heat fluxes for water are normally considered
to start around 0.4×10^6 Btu/hr ft^2, however, the authors
have shown values of half this amount under low pressure
conditions.

Beaver and Hughmark [9] conducted experiments
on twelve fluids in a 3/4 in. by 8-ft long carbon steel
tube, heated electrically, to investigate the reliability
of using developed correlations invacuum operations. It
was concluded that for wall minus saturation temperature

differences less than 15°F, single phase coefficients domi-
nate and can be predicted by a modified Dittus-Boelter
equation (Sieder-Tate modification):

$$Nu = 0.023(Re)^{0.8}(Pr)^{0.4}(\mu_L'/\mu_W)^{0.14} \qquad (2.6)$$

For temperature differences greater than 15°F nucleation
sets in and local inside coefficients can be predicted by
existing two-phase correlations.

Shellene et al. [10] carried out plant tests
on a highly instrumented 110 ft^2 reboiler having a 14-in.
shell, containing 70 3/4 in. 13 gauge, 3 7/8 in., 12
gauge, 8-ft long tubes. The reboiler was operated in conjun-
ction with an existing distillation column and, except for
instrumentation, was identical to a typical commercial unit.
Steam was used as the heat source and the process fluids were
benzene, water, isopropyl alcohol, methyl ethyl ketone, glycerine,
and various aqueous solutions of the alcohol, ketone, and
glycerine. The process pressure was slightly above atmos-
pheric. Of particular interest in the work was the explora-
tion of the onset of unstable operation.It was found that
the addition of flow resistance to the inlet line extended
the stable operating range, and the allowable pressure drop
across the tubes decreases as the heat flux increases. Adding
flow resistance to the vapour return line results in a decre-
ase in the maximum flux. The authors recommend to keep the

return line flow area atleast equal to the total flow area of the tubes. Maximum heat fluxes are tabulated for the various fluids with accompanying temperature differences and per cent vaporisation. Other data are presented as heat flux versus log mean temperature difference and mass velocity versus pressure drop.

Takeda et al. [11] meadured the axial distribution of vapour holdup and boiling heat transfer coefficient in the annuli of a natural circulation vertical tube evaporator for pure liquids (water, methanol) and liquid mixtures (10 mole % methanol - water, 50 mole % methanol water, 100 g/lit. H_2O -$C_{12}H_{25}C_2H_4SO_3$ - Na). Vapour hold up in the annuli is expressed in terms of heat transfer rate and length of boiling region. The effect of vapour holdup on the boiling heat transfer coefficients is analysed to give an empirical dimensionless equation.

Chexal and Bergles [12] studied the stability characteristics of a single-channel vertical thermosiphon reboiler. The test section consisted of electric-resistance heated glass tubing . The glass tubing was 70% optically transparent, hence visual observation of the two phase flow processes was possible. Seven steady and fluctuating flow modes were observed for a wide range of inlet sub-cooling and heat flux. Flow regime maps were developed in terms of these coordinates for both water and Freon-113

for a variety of inlet and exit valve settings.

Calus-et al. [13] carried out experimental work
on a single tube natural circulation reboiler to investi-
gate heat transfer to single component liquids . One copper
and one stainless steel tube each equipped with a single
steam jacket, and one stainless steel tube equipped with a
six-compartment steam jacket were used. All the tubes had
nominal dimensions of 0.5 in. diameter, and 48 in. height.
Three workers worked independently to obtain the length
mean and local point coefficients of heat transfer for
water, isopropanol, n-propanol and their azeotropes. Two-phase
heat transfer coefficients for all five liquids were corre-
lated by a single equation :

$$\frac{h_{TP}}{h_L} = 0.065 \left(\frac{1}{X_{tt}} \right) \left(\frac{T_s}{\Delta T} \right) \left(\frac{\sigma_{H_2O}}{\sigma_L} \right)^{0.9} \quad (2.7)$$

All the length mean coefficients from runs with a two-phase
mixture quality of between 0.02 and 0.68 at the tube exit
are correlated well within the $\pm$ 20 % accuracy limits. The
same equation correlates point heat transfer coefficients
from runs with a quality in the range of 12% to 50% within
$\pm$ 30% accuracy limits. The dimensionless groups ($\frac{T_s}{\Delta T}$)
and ($\frac{\sigma_{H_2O}}{\sigma_L}$) are powerful correlating factors. The latter
group accounts for the differences in the nucleating proper-
ties of the various single component liquids and its correla-
ting effectiveness indicates that nucleation is one of the
mechanisms present in flow boiling.

Calus et al. [14] obtained heat transfer data from a natural circulation single tube reboiler for binary liquid mixtures of isopropanol, n-propanol, and glycerine each with water. Two tubes, one of copper and one of stainless steel, were used to obtain length mean heat transfer coefficients. Also one stainless steel tube was used to obtain local coefficients. All the three tubes had nominal dimensions of 0.5 in. diameter and 4-ft. length. It was found, in correlating the experimental data, that the single component correlation of [13] is adequate provided that the surface tension used in it is that of the binary liquid of the interfacial concentration σ_L^*, and that the temperature driving force is the difference between the wall temperature and the saturation temperature of the mixture of the interfacial concentration. The latter is found by correcting the apparent temperature difference ΔT with the correction factor F. The length mean coefficients corresponding to a combination of flow boiling, regimes, excluding the purely bubbly-nucleate and dry wall regimes, are correlated by the equation

$$\frac{h_{TP}}{h_L} = 0.065 \left(\frac{1}{X_{tt}}\right)\left(\frac{T_s}{\Delta T}\right)\left(\frac{\sigma_{H_2O}}{\sigma_L^*}\right)^{0.9} F^{0.6} \quad (2.8)$$

where the factor

$$F = \left[1 - (y^*-x)\left(\frac{C_L}{\lambda}\right)\left(\frac{\alpha}{D}\right)^{0.5}\left(\frac{dT}{dx}\right)\right] \quad (2.9)$$

75% to 95% of the data points, depending upon the type of

mixture , are within $\pm$ 20% accuracy limits. The same equation correlates the local coefficients within $\pm$ 30% accuracy limits if some of the data points, where nucleate boiling or dry wall regimes are suspected, are rejected. The factor F is a powerful parameter with binary mixtures having a highly non-ideal vapour-liquid equilibrium relationship. In the case of binary mixtures of low relative volatility this factor is very close to unity.

C H A P T E R   3

EXPERIMENTAL   INVESTIGATION

3.1   EXPERIMENTAL SET-UP

The test apparatus used in the present investiga-
tion was a single tube vertical thermosiphon reboiler desi-
gned for distilled water and water-glycerine mixtures.
The unit mainly consisted of a test section, a separator,
condensers, and a cooling jacket. The overall layout of
the experimental setup is shown photographically in Figure
3.1 and schematically in Figure 3.2.

3.1.1 Test Section

The test section formed a part of the thermosiphon
loop connected to the separator and a cooling jacket. It
was a vertical copper tube of 19.05 mm inside diameter and
1.58 mm thick. The heating length of the tube was 940 mm.
At the upper and lower ends of the test section, glass
tubes of 19 mm inside diameter were connected through
gland and nut arrangements. The glass and copper tubes
were carefully aligned. The glass tube at the upper end
of the test section helped in the visual observation of
flow pattern of the boiling liquid emerging out of the tube.
The lower end glass tube provided a view of the entering
liquid. The exit end of the thermosiphon loop was finally
connec ted to the side of a vapor-liquid separator through
a cup mixing device as shown in Figure 3.2. The cup mixing
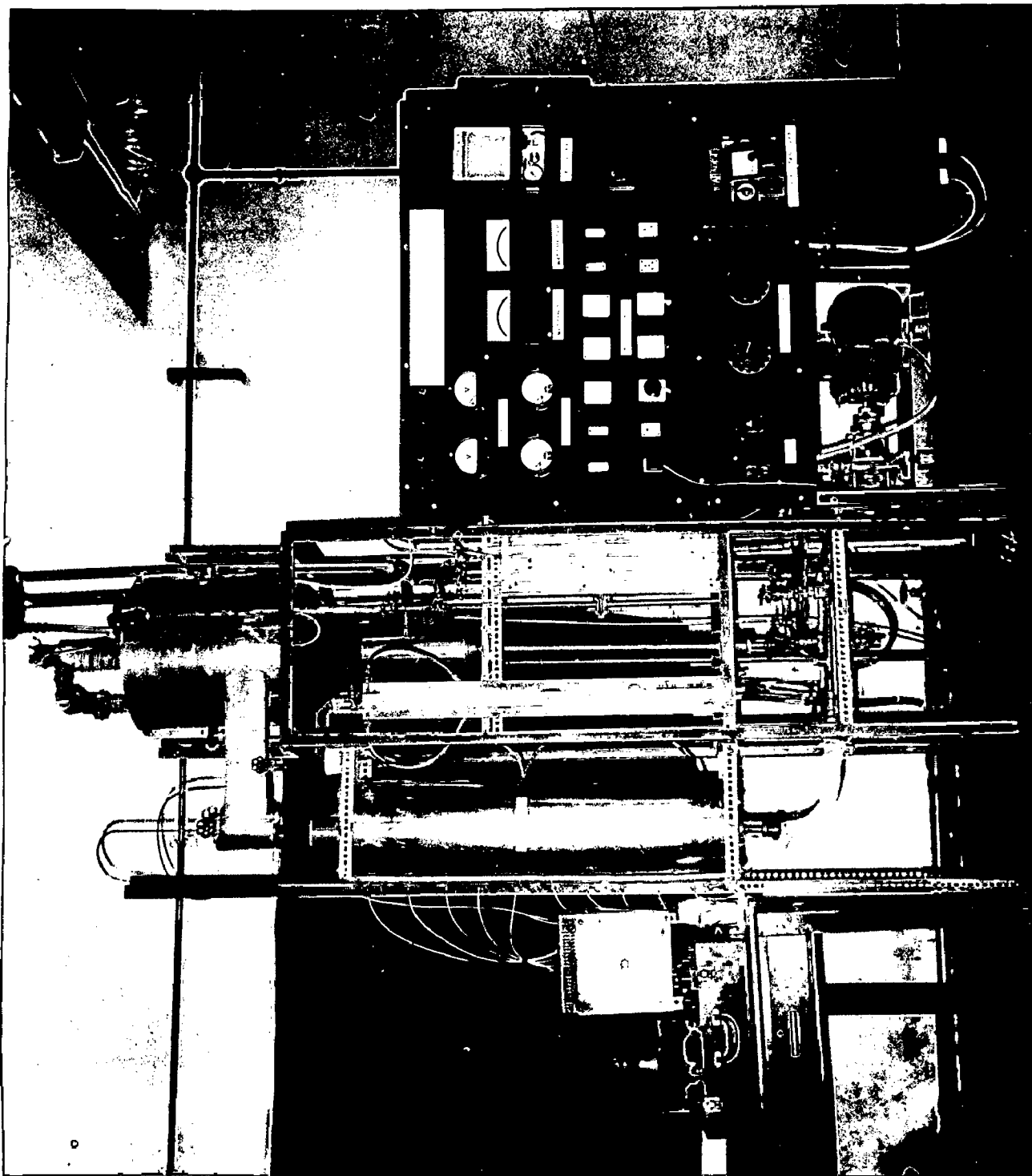
Fig. 3·1 Overall apparatus layout

1 – Test Section
2 – Wall Thermocouples
3 – Liquid Thermocouples
4 – Glass Tubes
5 – Cooling Jacket
6 – Cooling Water Line
7 – Liquid Level Indicator
8 – Separator
9 – Condensers
10 – Air Vent
11 – Cupmixing Device
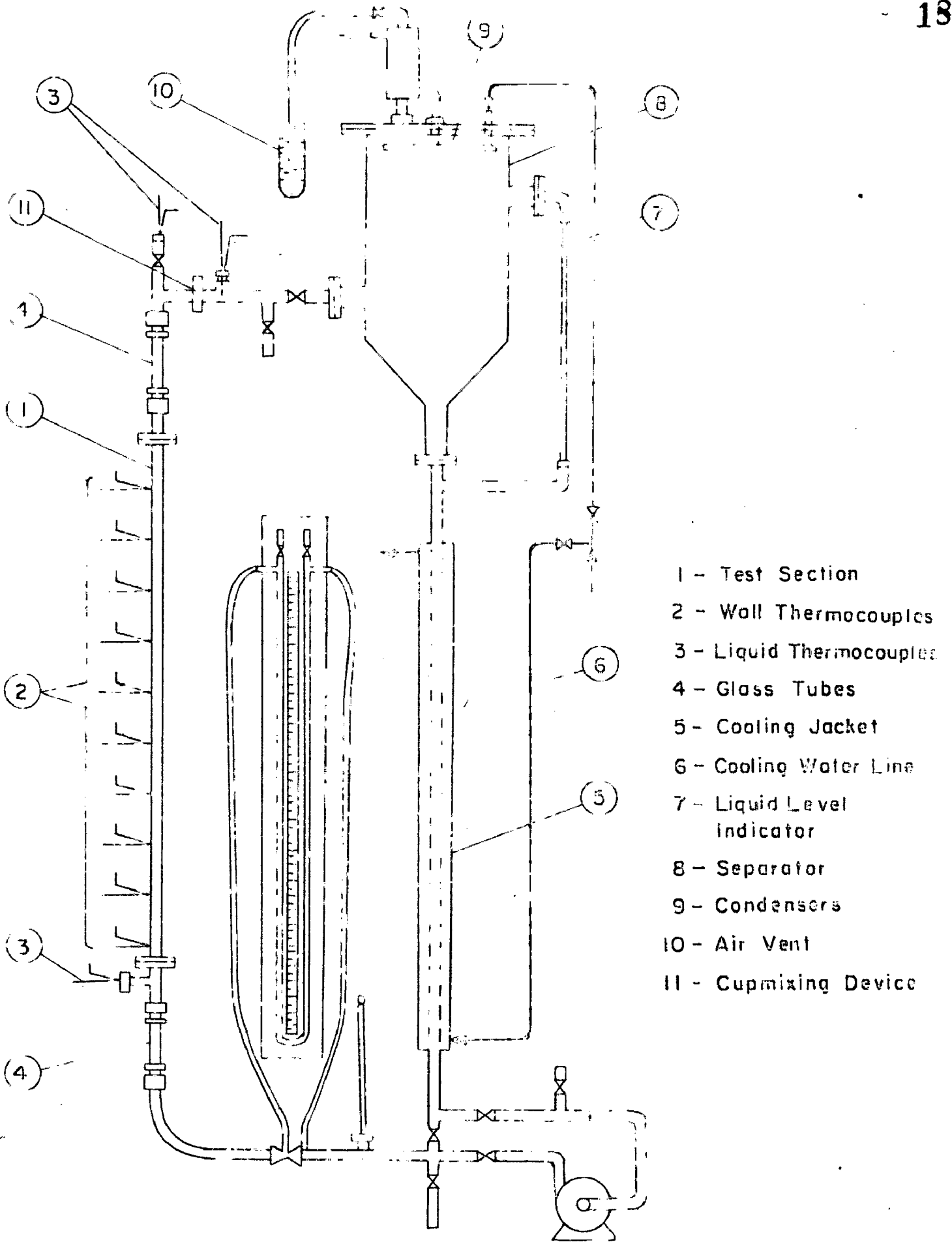
Fig. 3·2 Schematic diagram of experimental set-up

device was used to homogenise the liquid temperature, before it is measured by the liquid thermocouple probe, in order to get the bulk liquid temperature. The lower end of the loop was connected to the conical bottom of the separator through a flow meter and a cooling jacket.

The test section was heated externally by an electrical heating element. The heating element was made of Nichrome wire (22 gauge) of 3.48 Ohm/m resistance wound on the copper tube. Porcelain beads of a suitable size were used over the nichrome wire for electrical insulation. The terminals of the heating element were screwed to especially designed brass rings which were fitted on the tube. Mica sheet was used to insulate the brass rings from the copper tube. The test section was lagged thoroughly with glass wool insulation and wrapped with thin aluminium sheet. The power supply to the heating element was stabilized by means of a voltage stabilizer. The energy input to the element was regulated by means of auto-transformers and was measured by calibrated wattmeters.

The aim of the present study was to measure the local heat transfer coefficient at various positions in the tube as the liquid boils and rises up under thermosiphoning effect. The local coefficient can be computed using the measured local values of heat flux and temperatures in the following equation :

$$h_z = \frac{q'}{t_W - t_L}$$
(3.1)

It was, therefore, essential to measure the temperatures of heat transfer surface and liquid accurately. This was done by means of copper constantan thermocouples (Gauge 24).

The temperature of the heat transfer surface was measured at 10 locations, at intervals of 100 mm starting from the lower end of the heated section. Thermocouple beads were imbedded in the tube wall and the leads were wound along the circumference before they were taken out to the e.m.f measuring system. The measured temperatures directly represented the inside surface temperature because the temperature drop between the thermocouple bead location and the inner surface of the tube was negligible (Appendix D.1). The inlet liquid temperature was recorded by a thermocouple probe inserted just before the heating section at the lower end of the tube. The thermocouple probe fitted just after the cup mixing device measured the bulk liquid temperature of outgoing liquid. A travelling thermocouple probe was inserted axially into the tube from the top to register the liquid temperatures along the tube at positions corresponding to those of wall thermocouples . The local liquid temperatures , however, could be measured only in the upper half of the test section length. The presence of the thermocouple probe at the axis of the tube is likely to alter the flow pattern and thus affect

the experimental data. To safeguard against this source of error, the probe was lifted up and was kept out of the flow path during normal course of operation. After all the readings of wall and liquid temperatures were taken, the probe was lowered and local liquid temperatures were recorded quickly starting from the upper most position. By the above procedure, thus, the effect of presence of thermocouple probe on experimental data was found to be negligible. All the thermocouples were connected to the potentiometer through a selector switch and cold junction. The cold junction was maintained at $0^{\circ}C$ by dipping it in melting ice bath. The e.m.f of thermocouples was measured by means of a vernier potentiometer with a sensitive spot galvanometer. This arrangement made it possible to measure e.mf. upto 0.001 mV with an accuracy of 0.01 per cent.

3.1.2 Separator

The vapour-liquid separator was a cylindrical vessel of 282 mm inside diameter and 425 mm long with a conical bottom and a flanged top cover. It was made of aluminium. The exit end of thermosiphon loop was connected to the side of the vessel near the conical bottom. The bottom of the separator was connected to the inlet end of thermosiphon loop through a jacketed pipe. The two-phase mixture from the test section entered the vessel and got separated into liquid and

vapour phases. The liquid moved down to the cooling
jacket whereas the vapor went up towards condensers.
A level indicator was fitted to the separator to observe
the liquid level in the bottom of separator. This also
provided the initial liquid level in the test section.
The separator was insulated thoroughly with glasswool insu-
lation and was wrapped with thin aluminium sheet.

3.1.3 Condensers

The ascending vapors from the separator were
condensed by two surface condensers and returned to the
circulating liquid. The internal condenser consisted of
a spiral coil made of 12.5 mm diameter copper tube. The
coil was kept just below the top cover of seperator. The
inlet and outlet ends of the coil were taken out through
the cover. A jacketed copper tube of 20 mm diameter served
as external condenser. The external condenser, in series
with the internal condenser, was fitted to the top of
the separator. Water was used as cooling medium and
was supplied to the condensers from a constant level tank.
The free end of the jacketed tube was provided with a
drain cock and a polythene tube was connected to it.
The other end of the tube was kept submerged in water.
This air vent arrangement helped in the visual observa-
tion of removal of last traces of dissolved air from
the test liquids.

-

ta

g

e

do

c

ument.

3.1.4 Cooling Jacket

A cooling jacket was fitted on the vertical tube connecting the bottom of separator and inlet portion of circulation loop. Cooling water to the jacket was supplied from a constant level tank. The inlet temperature of test liquid could be adjusted and controlled at a desired value by regulating the water flow rate to the jacket.

In between the vertical jacketed tube and horizontal inlet portion of natural circulation loop, was connected an auxiliary forced circulation loop consisting of a centrifugal pump and its suction and discharge lines. The pump was provided to conduct the experimental study of forced convective heat transfer which served as standardization of the apparatus.

3.2 EXPERIMENTAL PROCEDURE

3.2.1 Performance of Thermocouples

Performance of all the wall and the liquid thermocouples installed in position was examined. Water-glycerine solution (20 wt.%) was filled upto a level in the separator to ensure complete submergence of circulation loop. A standard mercury in glass thermometer was placed in the liquid. The liquid was heated by an immersion heater in the separator and was circulated through the test section. The liquid temperature was raised to a particular value and was maintained by means of the cooling

jacket. Sufficient time was allowed for establishing the thermal equilibrium between liquid and tube wall, and readings of thermocouples and thermometer were noted. Similar runs were taken at different liquid temperatures and are reported in Table A.1 The data show a maximum deviation of 0.15 per cent in temperatures measured by the thermometer and thermocouples.

3.2.2 Calibration of Wattmeter

The wattmeters used for the measurement of electrical energy input were calibrated against a substandard wattmeter, BS-89 Grade Pr supplied by M/s Cambridge Industrial Co. Ltd., London. The calibration readings as given in Table A.2, show a maximum deviation of 1.7 per cent.

3.2.3 Heat Balance and Standardization of Apparatus

Experimental runs were taken to check the heat balance on the test section and are reported in Table A.4 Water was allowed to flow through the test section at a constant rate and a suitable heat flux was adjusted. The exit water was allowed to drain away to give a once through operation. After the steady state was reached, the readings of flow rate, wattmeters and thermocouples were recorded. The energy balance calculations indicated a maximum deviation of 1.5 per cent in heat balance.

The calculation of Reynolds number indicated the laminar flow conditions in the tube and heat transfer took place

by mixed convection-forced convection influenced by natural convection. The equation of Sieder and Tate [15] with correction factor for free convection is applicable for such a situation.

$$Nu = \left[1.86 \left[Re \times Pr \times \frac{d}{z} \right] \right]^{1/3} \left(\frac{\mu_L}{\mu_W} \right)^{0.14} \chi$$

(3.2)

where

$$\chi = 2.25 \frac{\left[1 + 0.01(Gr)^{1/3} \right]}{\log Re}$$

The experimental values of average heat transfer coefficient were compared with those predicted by using Eq.(3.2) A maximum absolute deviation of 11.35 per cent indicated that the experimental technique and measurements would generate reliable experimental data of acceptable standard.

3.2.4 Operating Procedure

After the fabrication and assembly of the apparatus was completed, it was tested for leaks which were rectified. The circulation system and the separator were flushed with water and cleaned by circulating water with the help of pump. The electrical and thermocouple connections were made and performance of measuring system was examined. A few runs were taken to check the heat balance and reliability of experimental data. The pump was

then disconnected from the circulation loop by closing the valves of the suction and discharge lines and the system was filled with distilled water upto the top of the test section. The apparatuswas run for several days to obtain the stable tube wall nucleating characteristics. When the wall temperatures ceased to change further with time under identical operating conditions, the main experimental runs began . During the start up of reboiler operation to conduct a series of runs, the test liquid was boiled for about an hour to drive out any dissolved air from the liquid. The removal of the traces of air was ensured when the air bubbles ceased to come out of the air vent. A heat flux was then adjusted by means of auto-transformers. The water flow rate to the cooling jacket was adjusted to get the desired degree of subcooling at the inlet of test section. The cooling water to the condensers was kept running throughout the experimentation. The steady state conditions were established after about $1\frac{1}{2}$ hours. The readings of wattmeters, wall thermcouple and liquid thermocouples at inlet and outlet of test section were recorded. The moving thermocouple was lowered and liquid temperatures corresponding to wall thermocouple positions were noted. The local values of liquid temperatures for distilled water could also be predicted from the trend of local wall temperatures. A good agreement between the measured and predicted liquid .

temperatures was observed. Such a prediction of liquid
temperatures was not possible for water-glycerine mixtures.
Similar runs were taken at different heat fluxes and degrees
of subcooling.

Experimental data were collected for water and
four water-glycerine mixtures of 20.90, 43.25 , 62.75
and 86.50 wt.% water compositions. The heat flux ranged
from 8.88×10^3 to 24.88×10^3 W/m^2. With the layout
designed for a closed system operation and with stabilized
power supply, the apparatus once charged and started could
be left running even unattended for hours without any change
in the liquid submergence or mixture composition.

-- --

C H A P T E R 4

RESULTS AND DISCUSSION

In this chapter, the results of experimental measu-
rements on heat transfer during boiling of water and water-
glycerine mixtures at atmospheric pressure in a single tube
natural circulation reboiler have been discussed. The study
included the measurement of wall and liquid temperature dis-
tributions along the length of the tube for various degrees
of subcooling and heat fluxes. From this information the
local values of transfer coefficients are computed and
their dependence on various parameters is examined.

Table 4.1 shows the ranges of experimental para-
meters investigated.

Table 4.1   Range of Experimental Parameters

System	Composition wt.% water	Degree of subcooling at inlet of tube $^{\circ}C$	Heat flux W/m^2
Water	100	4.2 - 43.63	10.66×10^3 - 24.88×10^3
Water - glycerine	20.90, 43.25, 62.75, 86.50	5.13 - 46.44	10.66×10^3 - 24.88×10^3

Low heat flux values were used in the present
investigation, in order to cover the single phase natural
convection, subcooled boiling and fully developed saturated

boiling regions in the tube. The experimental data are tabulated in Appendix B.

4.1 HEAT TRANSFER DURING NATURAL CIRCULATION BOILING OF WATER IN A VERTICAL TUBE

4.1.1 Variation of Wall and Liquid Temperatures along the Tube Length

Figures 4.1 and 4.2 represent typical plots of wall and liquid temperatures versus distance along the test section from its lower end at different degrees of subcooling at inlet and various values of heat fluxes for water.

On examining these figures, the following points may be noted :

a. The wall temperatures, t_w start changing with decreasing slopes which eventually become constant resulting in a linear variation of t_w with positions along the tube from its inlet. The linear variation of t_w continues upto a certain position followed by a decreasing slope which finally passes through zero to negative slopes resulting in the decrease of wall temperatures approaching constant values.

b. The liquid temperature t_L varies linearly with distance along the test section upto a point beyond which it ceases to change. The point marks the beginning of the section where both wall and liquid temperature curves becomes almost horizontal. The value of liquid temperature corresponding to the horizontal portion of curves was the saturation temperature of liquid.
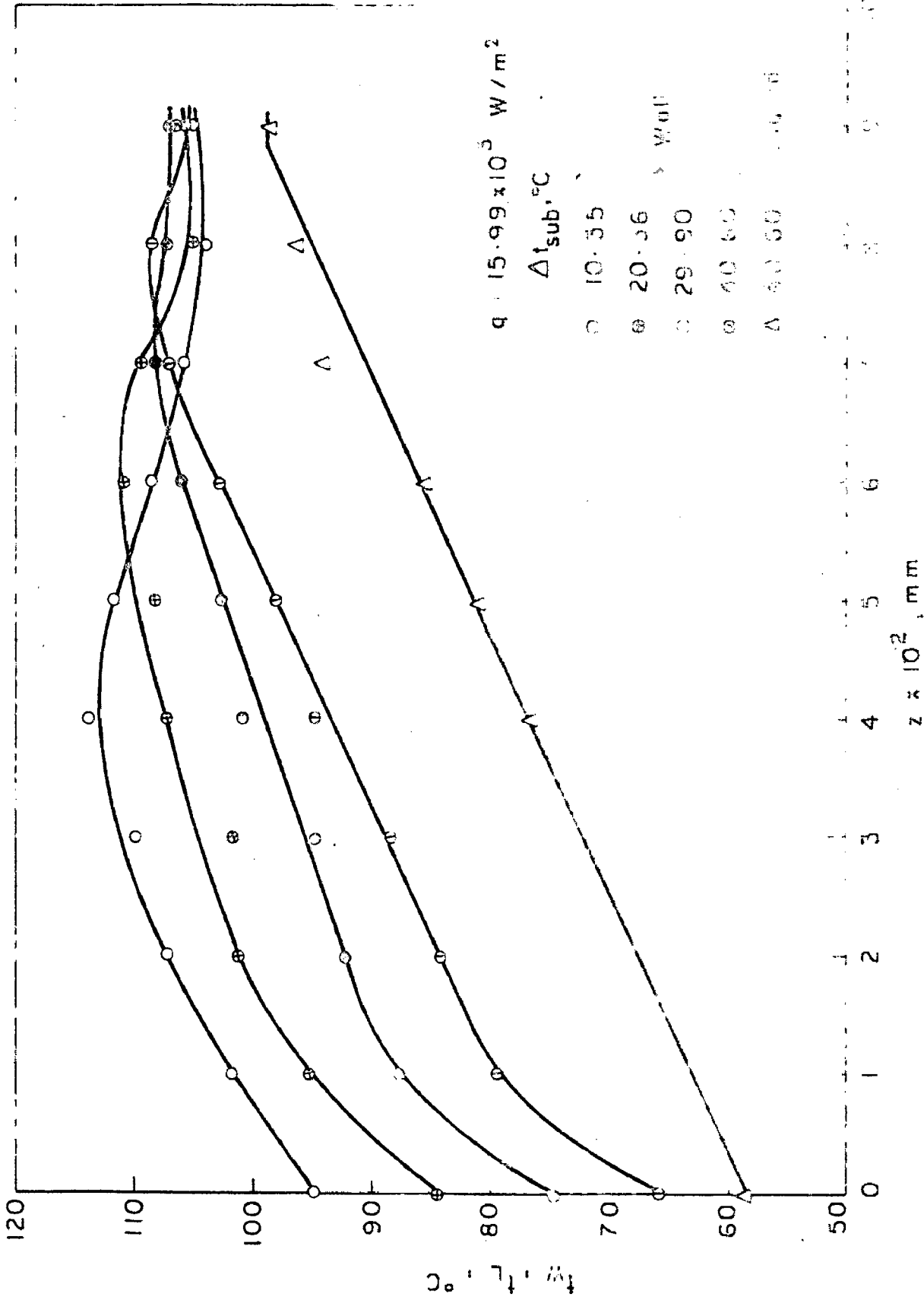
Fig. 4.1 Variation of liquid and wall temperatures along the tube length at a constant q and various Δt_{sub} for water
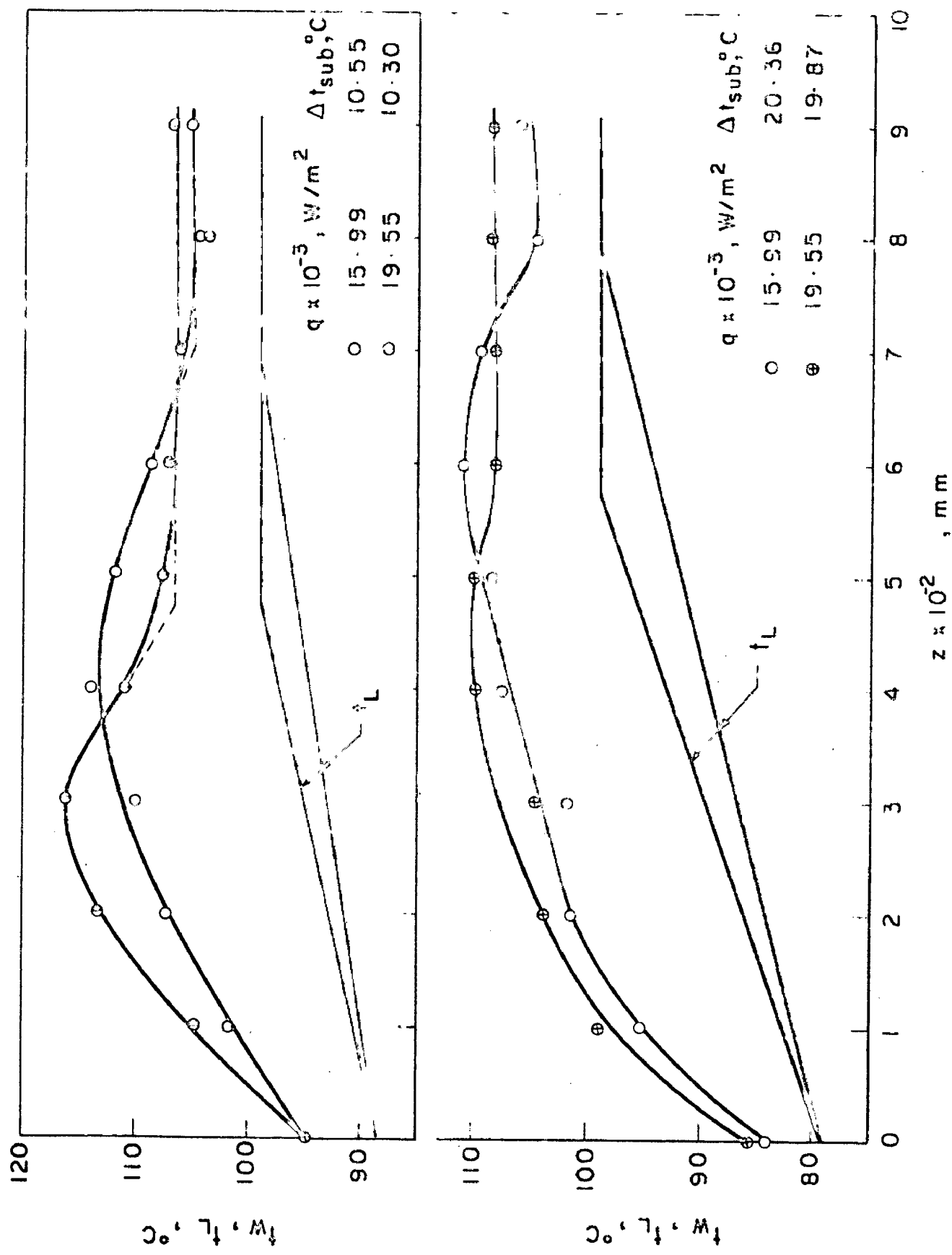
Fig. 4.2 Variation of wall and liquid temperatures along the tube length for various q and Δt_{sub} for water

c.   At lower values of Δt_{sub}, the curves are found
to have essentially the same characteristic features
but the horizontal portion of the curves is stretched
and the portions of wall temperature curves with chan-
ging slopes are shifted to the left reducing the linear
portions.

d.   With the rise in the value of heat flux, the wall tem-
peratures shift to higher values with longer horizontal
portions and correspondingly smaller linear portions.

The above characteristic features of wall and liquid
temperature distribution are indicative of basic mechanism of
heat transfer in the test section. The initial portions of
the curves have wall temperatures increasing at faster rates
due to the entrance effects in the tube, with developing ther-
mal boundary layer. The linear variation of wall temperature,
almost parallel to the corresponding liquid temperature, indi-
cates the heat transfer by natural convection. The linear por-
tions extend even upto wall temperatures higher than the satura-
tion temperature of the liquid due to the requirement of a
minimum amount of degree of superheat for bubble formation as
observed in pool boiling investigations [16, 17] . The
value of this wall superheat in the present study is found
to be much higher than that in pool boiling studies presum-
ably because the process of bubble nucleation in the tube is
suppressed by the induced flow of liquid through the tube. The
points at which the curves deviate from the straight lines,

mark the onset of effective surface boiling. The bubbles, nucleate at the surface and create additional turbulence resulting in slow change of wall temperature. As the liquid rises up the tube, its temperature also increases linearly and bubbles can nucleate and grow to bigger size making the boiling process increasingly effective. This explains the subsequent decrease in wall temperature. Once the liquid attains the saturation temperature, fully devéloped nucleate boiling sets in with the vapour existing as the second phase, the quantity increasing along the tube length. The rate of heat transfer in this region in effected by the nucleate boiling and convection. As the quantity of vapor increases along the tube length, and thereforethe fluid velocity, the effect of nucleation diminishes whereas convective heat transfer predominates. This seems to explain the horizontal portions of the distribution curves in figures 4.1 and 4.2.

With smaller values of Δt_{sub}, the wall temperature corresponding to minimum value of Δt_{sub} for bubble formation is attained at a lower position in the tube and thus the onset of surface boiling is moved downwards in the tube. The saturation temperature is also attained by the liquid at lower position shifting the point of fully developed nucleate boiling. At higher values of heat flux, the wall and liquid temperatures rise faster with tube length attaining the onset conditions at smaller

distances from the inlet of the heating section.

4.1.2 Variation of Heat Transfer Coefficient with Distance along the Tube Length

The local value of h has been plotted as a function of z with Δt_{sub} and q as parameters in Figures 4.3 and 4.4 respectively. The change in heat transfer coefficient is insignificant upto certain length beyond which it increases sharply. The almost horizontal portions of the curves represent single phase natural convective region whereas the latter parts indicate the nucleate boiling region. The nucleation of bubbles and their growth on the heating surface at reduced local degree of subcooling along the tube length explain the increase in the value of heat transfer coefficient. Decrease in Δt_{sub} shifts the curves to the left suggesting that at a given heat flux, higher heat transfer coefficients are obtained at any position in the tube if the inlet liquid temperature is raised. In Figure 4.4 it is observed that the curves shift to higher values of h with increase in the value of q. The increase in h with q during single phase natural convection is attributed to the rise in wall temperatures. In surface boiling, h increases with q due to the greater number of nucleation sites at the heating surface becoming active at higher value of q.
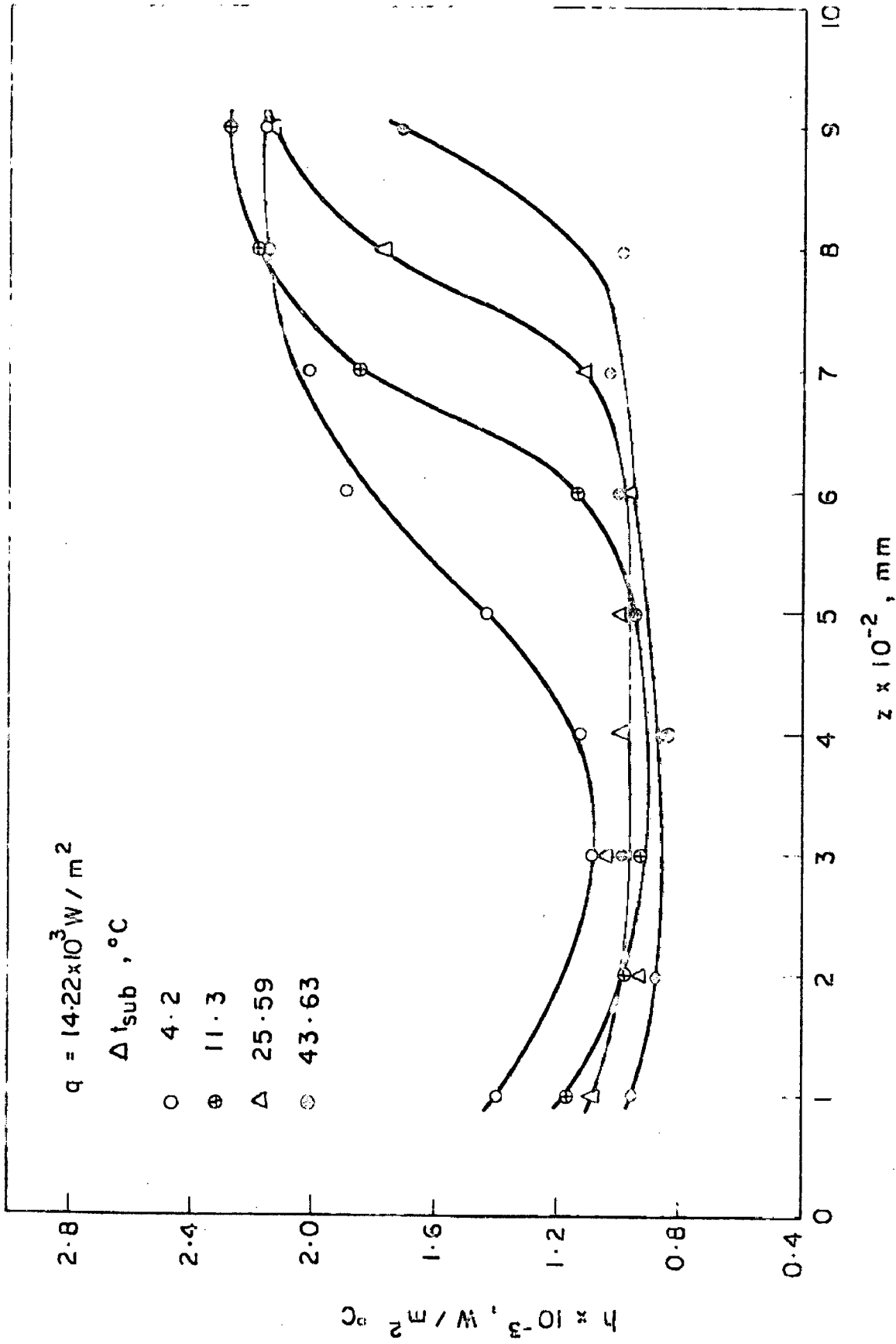
Fig. 4.3 Variation of h with z for a constant q and various Δt_{sub} for water
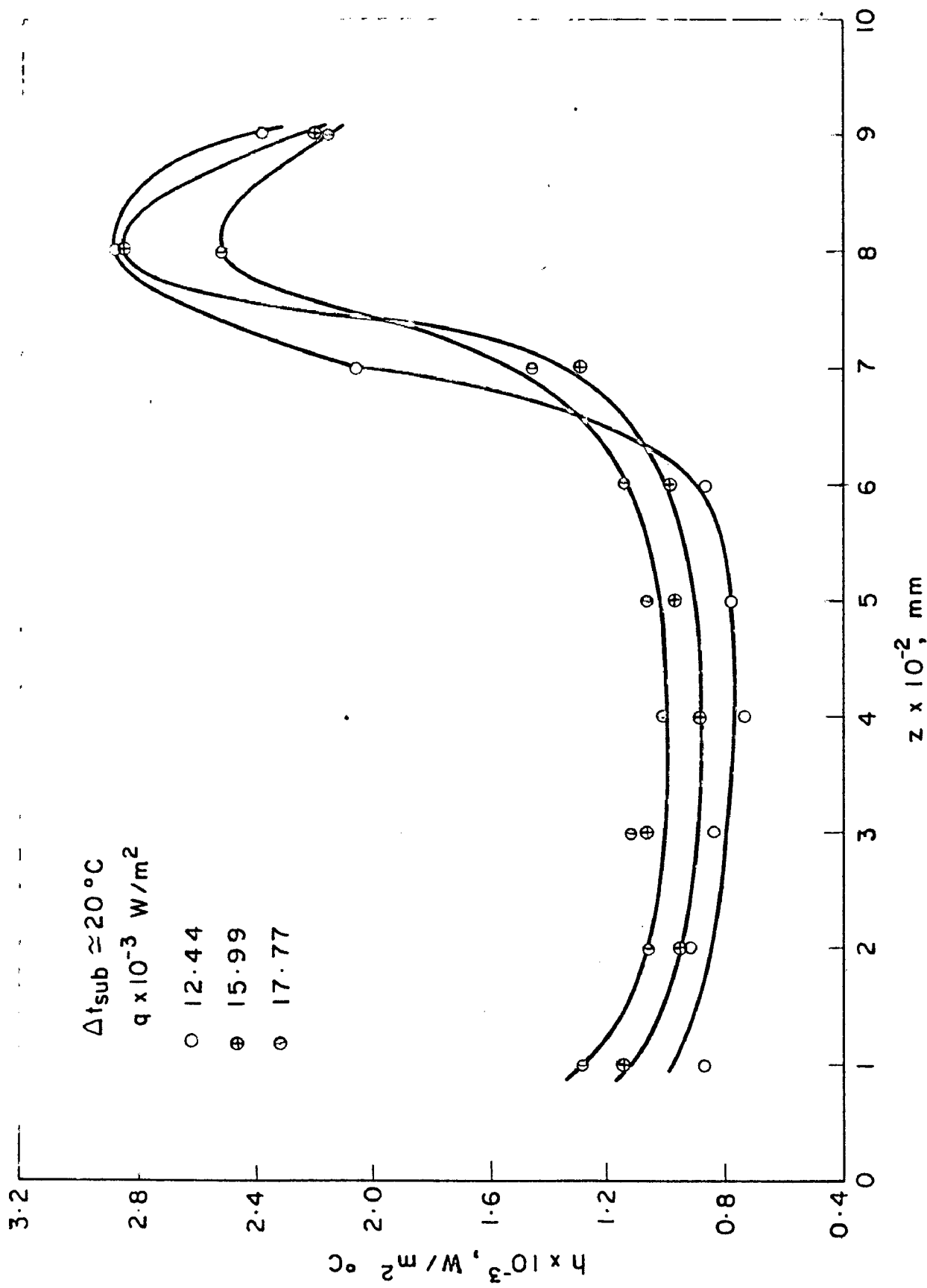
Fig. 4.4 Variation of h with z at various q and approximately same Δt_{sub} for water

The increase in heat transfer coefficient due to boiling along the tube length has been shown in Figure 4.5 as a plot of h_B/h_C versus z/d. It is observed from the figure that the local value of h in boiling rises at increasingly higher rates with tube length. The values of h_B/h_C are found to change markedly with Δt_{sub}.

4.1.3 Variation of h_B with q

The effect of heat flux on nucleate boiling heat transfer coefficient has been shown in Figure 4.6 on a log - log plot for three different levels of Δt_{sub}, at approximately 10,20 and 40^oC. The values of h_B are calculated at the onset of fully developed boiling where local degree of subcooling is zero and net generation of vapours begins. From this plot it is clearly seen that h_B increases linearly with q with a slope of 0.3. This value of slope is smaller than that in pool boiling (0.6 - 0.7) indicating that h_B increases at a lower rate as compared to the pool boiling conditions. This is quite an expected behaviour as the velocity of liquid in the tube suppresses the nucleation process.

4.2 HEAT TRANSFER DURING NATURAL CIRCULATION BOILING OF WATER-GLYCERINE MIXTURES IN A VERTICAL TUBE

4.2.1 Variation of Wall and Liquid Temperatures along the Tube Length.

Figures 4.7 and 4.8 show the typical plots of
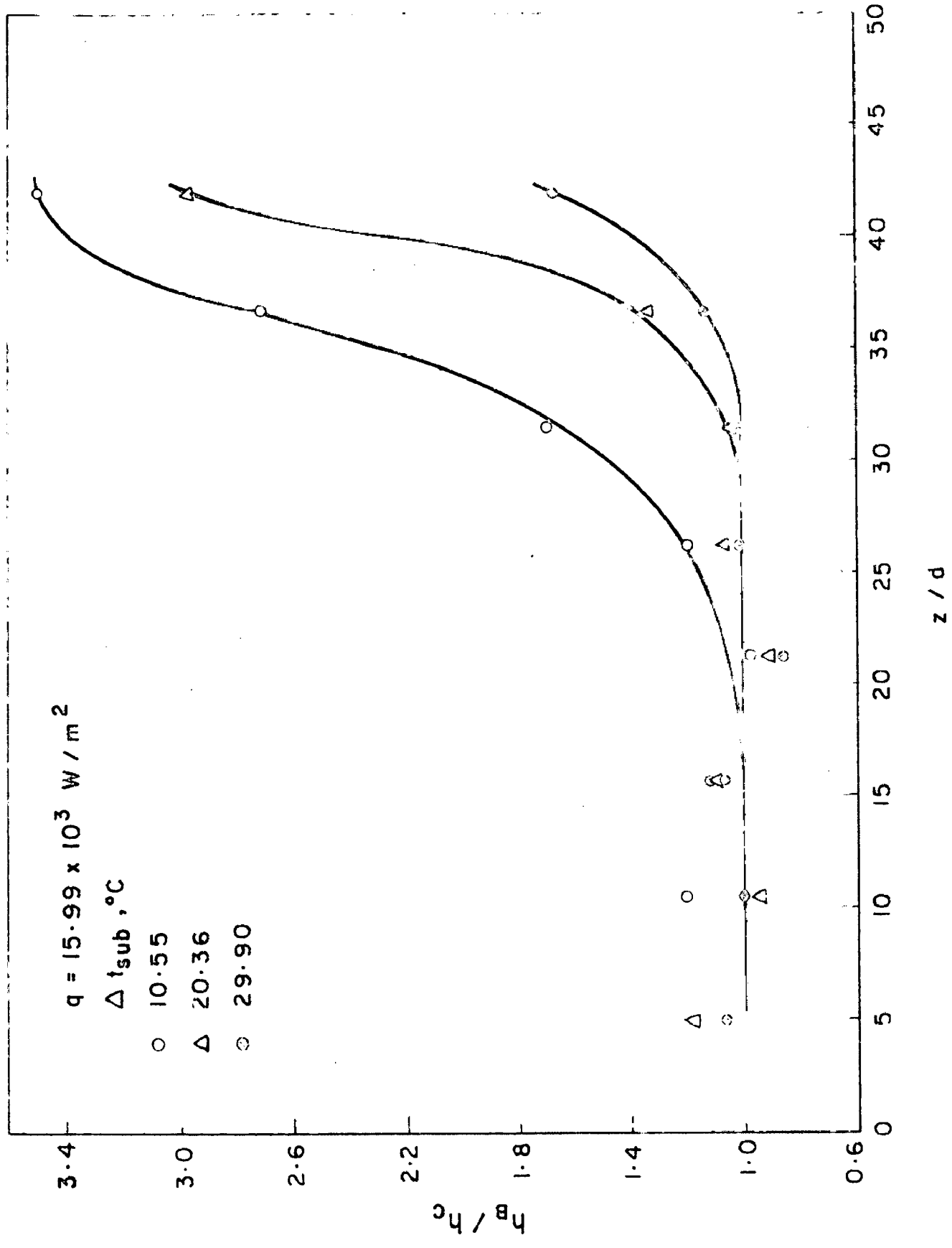
Fig. 4.5 Variation of h_B/h_C with z/d at different Δt_{sub} and same q for water
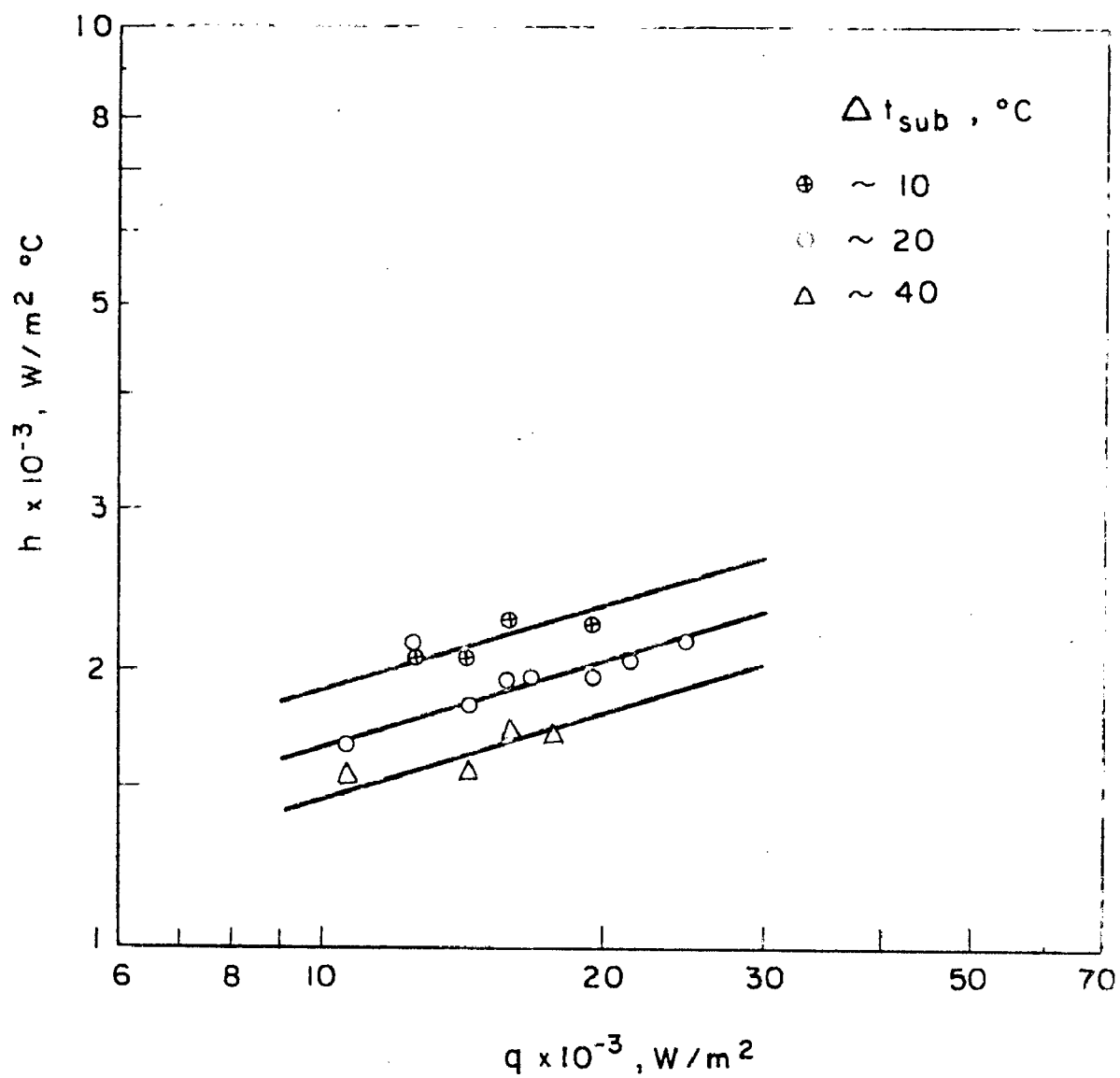
Fig. 4·6 Variation of h with q at the onset of bulk
          boiling of water
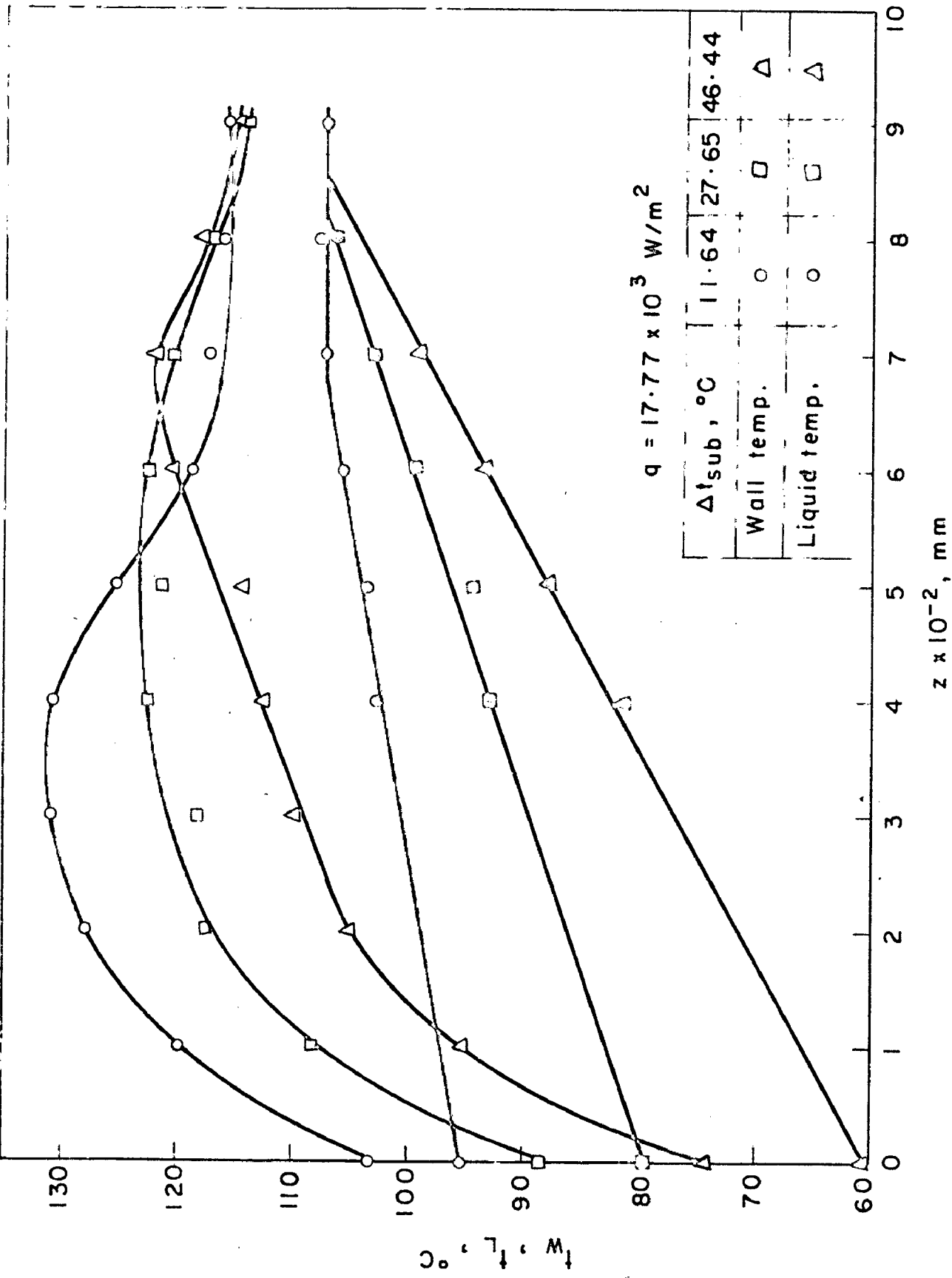
Fig. 4.7 Variation of wall and liquid temperatures along the tube length at constant q and different Δt_{sub} for 43.25 wt. % water-glycerine mixture
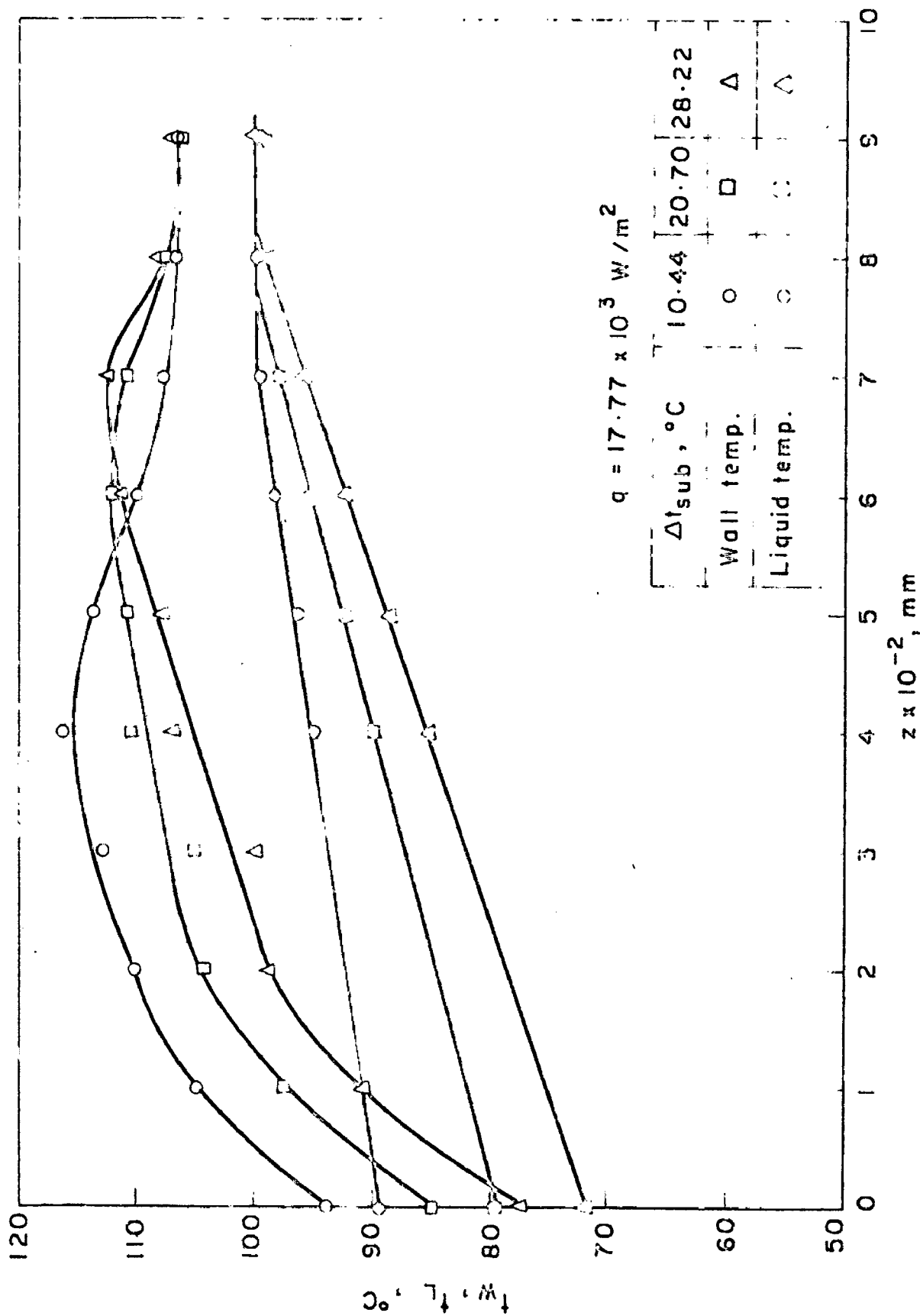
Fig. 4.8 Variation of wall and liquid temperatures along the tube length at constant q and different Δt_{sub} for 86.50 wt. % water-glycerine mixture

t_W and t_L versus z at a constant heat flux with degree
of subcooling as parameter for some compositions of water-
glycerine mixtures . It may be seen from these figures
that the wall and liquid temperature distributions along
the tube length for water-glycerine mixtures exhibit the
characteristic features essentially similar to those of
water as discussed in section 4.1.1.

In Figure 4.9 , the heat flux has been used as
parameter with approximately same value of degree of sub-
cooling of inlet liquid for 20.9 wt.% water-glycerine
mixture. The general behaviour of curves at all the heat
fluxes is almost the same. However, the increase in the
value of heat flux shifts the curves to higher values of
t_W.

4.2.2 Variation of Heat Transfer Coefficient with Distance
along the Tube Length.

Figures 4.10 and 4.11 show the plots of the dis-
tribution of heat transfer coefficient over the entire length
of the test section for different compoasitions of the mix-
ture. The general characteristics of the curves are similar
to those for water as discussed in section 4.1.2. Referring
to the Figure 4.10 it is noted that the curves are shifted
to higher value of h as the concentration of water in the
mixture is raised. This may be attributed to the change in
physical properties of the mixture with composition, in
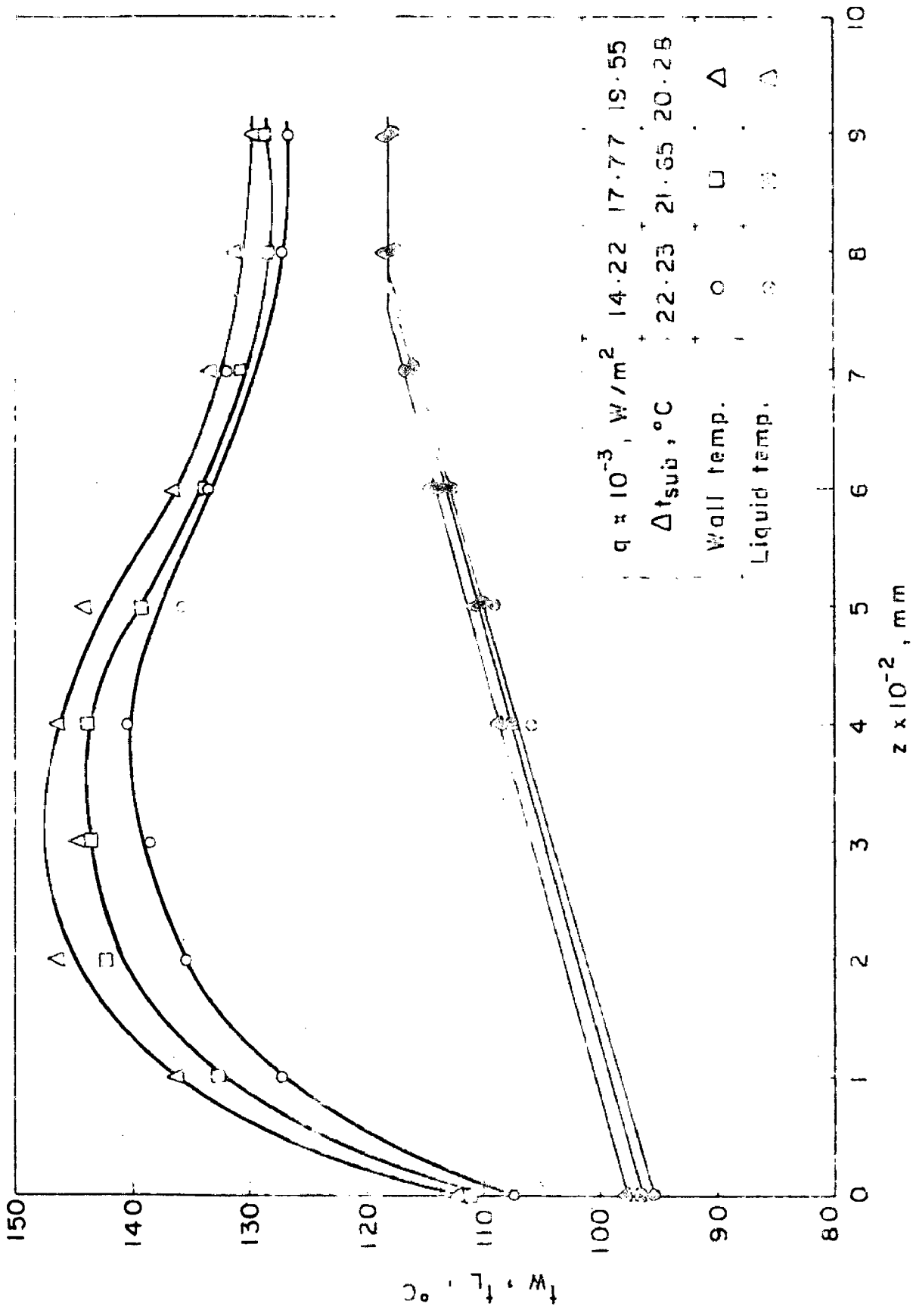
Fig. 4.9 Variation of wall and liquid temperatures along the tube length at approximately same Δt_{sub} and different a for 20.90 wt. % water-glycerine mixture
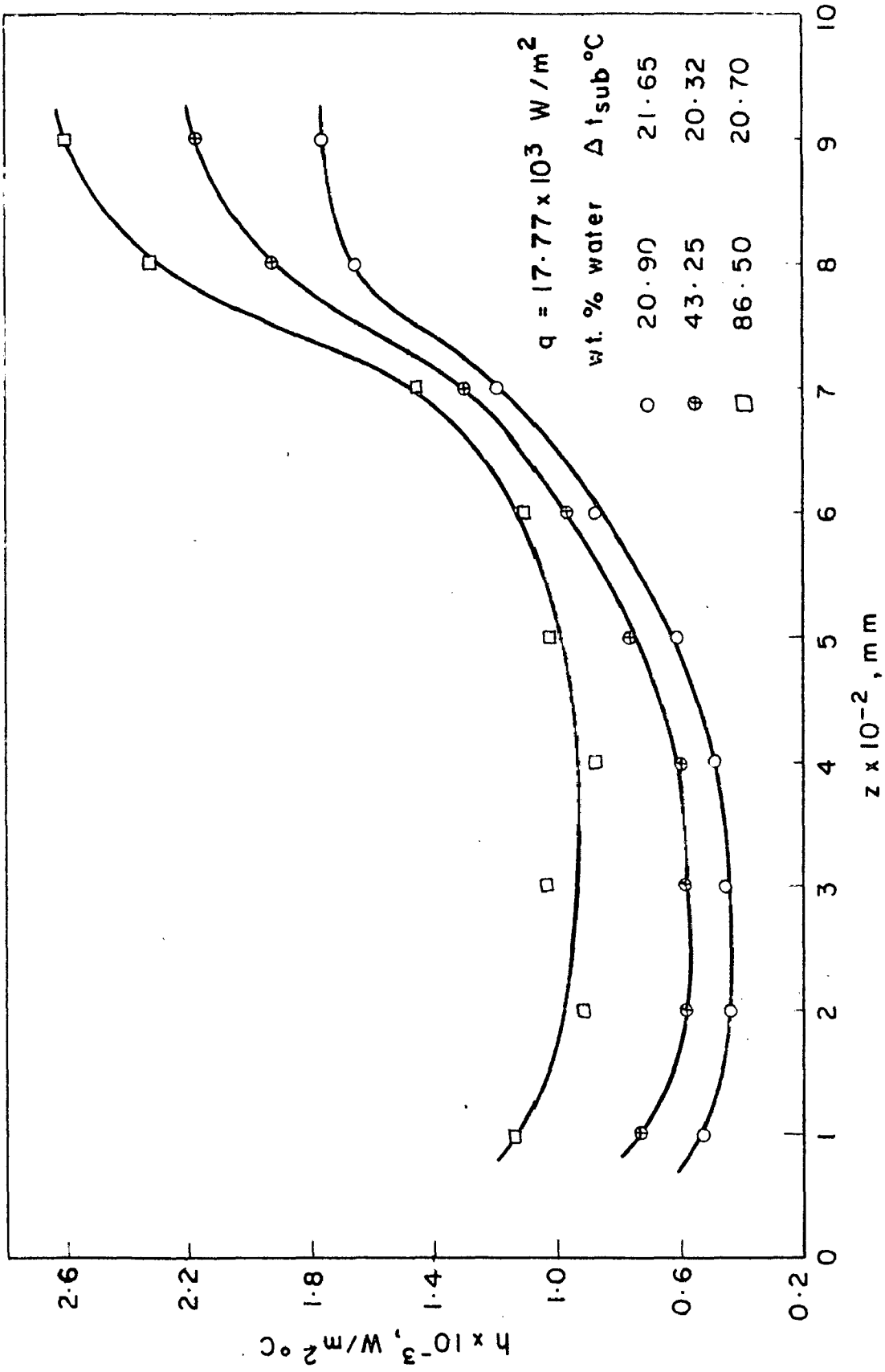
Fig. 4·10 Variation of heat transfer coefficient along the tube length at same q and Δt_sub for water-glycerine mixtures
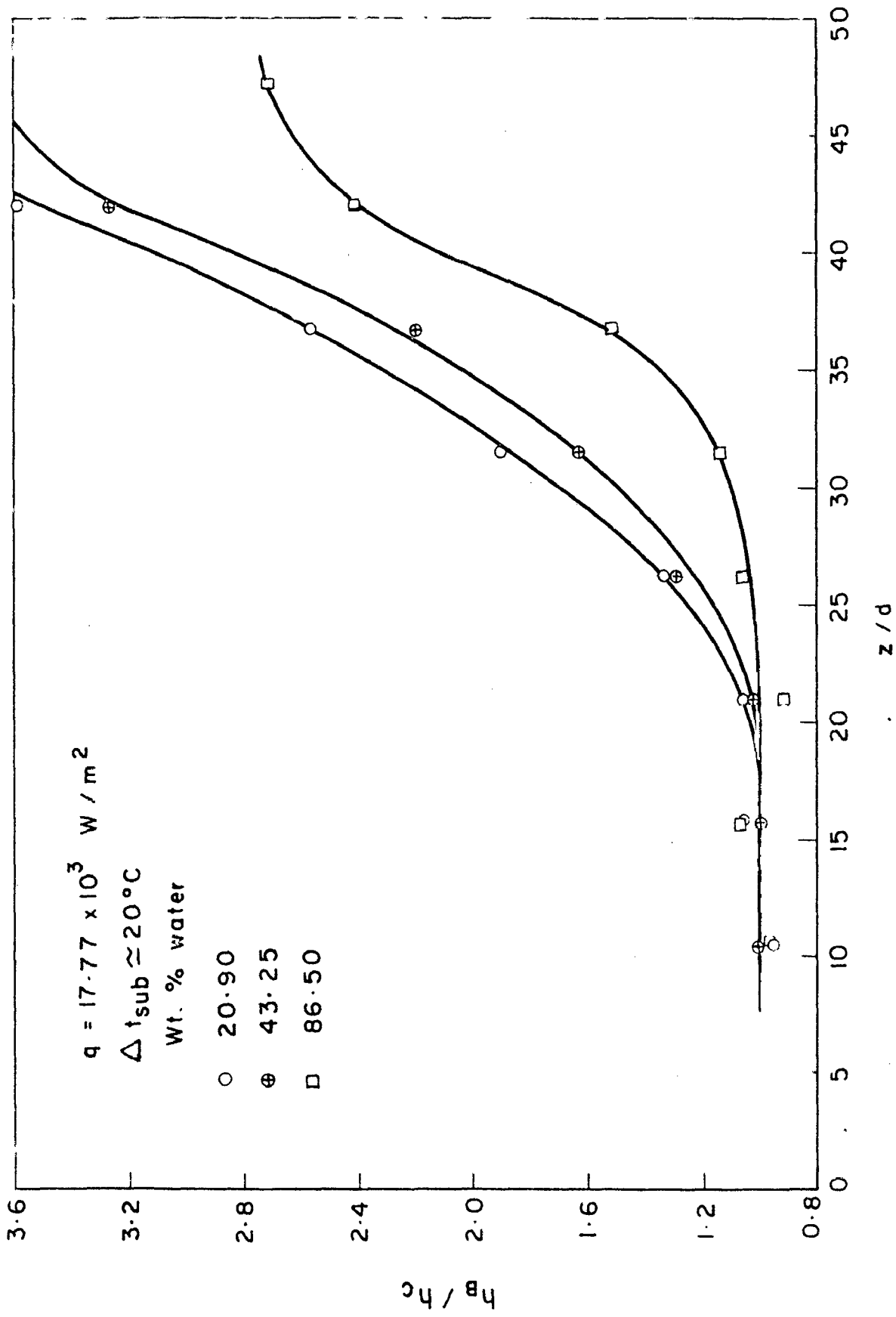
Fig. 4·11 Variation of h_B/h_C with z/d for water-glycerine mixtures

$q = 17·77 \times 10^3$ W/m²

$\triangle t_{sub} \simeq 20°C$

Wt. % water

O	20·90
⊕	43·25
☐	86·50

single phase natural convection region. The boiling heat transfer coefficient may be affected by mass diffusion in addition to the change in physical properties.

The results of Figure 4.10 have been replotted inFigure 4.11 showing the improvement in heat transfer due to boiling process. The ratio h_B/h_c rises slowly upto certain value of z/d beyond which a marked increase in the ratio is observed. Unlike the previous figure, the curves for higher wt.% of water shift towards the lower values of h_B / h_c at a given z/d. This may be explained by considering the variation of h_c with composition. The values of h_c depend strongly on the viscosity of liquid which decreases appreciably with increase in wt% of water for water-glycerine mixture. This results in a significant increase in h_c with wt.% of water in the mixture. The increase in the values of h_B is relatively less than that in h_c. As a result, the ratio h_B/h_c becomes smaller at higher concentrations of water in the mixtures.

4.3 GENERAL CORRELATIONS

The distribution of temperatures and heat transfer coefficients along the tube length under the effect of various parameters such as heat flux, degree of subcooling and mixture composition was examined in secstions 4.1 and 4.2. The results clearly indicated that there exist two distinct regions of heat transfer along the tube length :

a. Single phase natural convective region which
extends from the inlet of heating section to
a point where the tube wall attains a minimum
de-gree of superheat for effective surface
boiling to occur.

b. Boiling region consisting of surface boiling
and bulk boiling with bubble formation at the heat-
ing surface. This region occupies the remaining
portion of the tube.

4.3.1 Correlation of Heat Transfer for Single Phase
Natural Convection in a Vertical Tube

The average values of h_c for fully developed natu
ral convective region were found to depend on the temperature
drop across the film and physical properties of liquid at
mean bulk temperature. It was therefore argued to use the
Nusselt-Grashof-Prandtl type correlation, as it is generally
sought in other natural convective situations, in the follow-
ing functional form :

$$Nu = C_1 (Gr\ Pr)^{n_1} \qquad (4.1)$$

In order to account for the length of natural convec-
tive section a ratio of z_s/d was considered desirable. The
exponent of z_s/d was taken 0.5 as suggested by Lapin [18]
in a similar situation. A log-log plot of $Nu\ (d/z_s)^{0.5}$

versus (Gr Pr) was made as shown in Figure 4.12. From the average line passing through the data points the values of exponent, and constant, were determined to yield the following correlation

$$Nu = 3.33 \times 10^{-3} (Gr\ Pr)^{0.44} \left(\frac{z_s}{d}\right)^{0.5} \qquad (4.2)$$

Figure 4.13 shows the comparison between the experimentally measured values of Nu and those predicted by Eq. (4.2) . Almost all the data points for water and water-glycerine mixtures are found to show a reasonably good agreement within $\pm$ 20 per cent.

4.3.2 Correlation of Heat Transfer for Natural Circulation Boiling of Water in a Vertical Tube.

The heat transfer rate during boiling of liquid in tubes is governed by two types of convection processes:

a. Macroconvection due to the bulk flow of liquid through the tube.

b. Microconvection due to the bubble generation at the heating surface.

Before the onset of boiling process only the mac-roconvection exists and thus the ratio h_B/h_c represents the intensity of heat transfer in boiling. The value of h_B/h_c at any position in the tube, therefore, should depend upon the velocities responsible for respecstive convections.
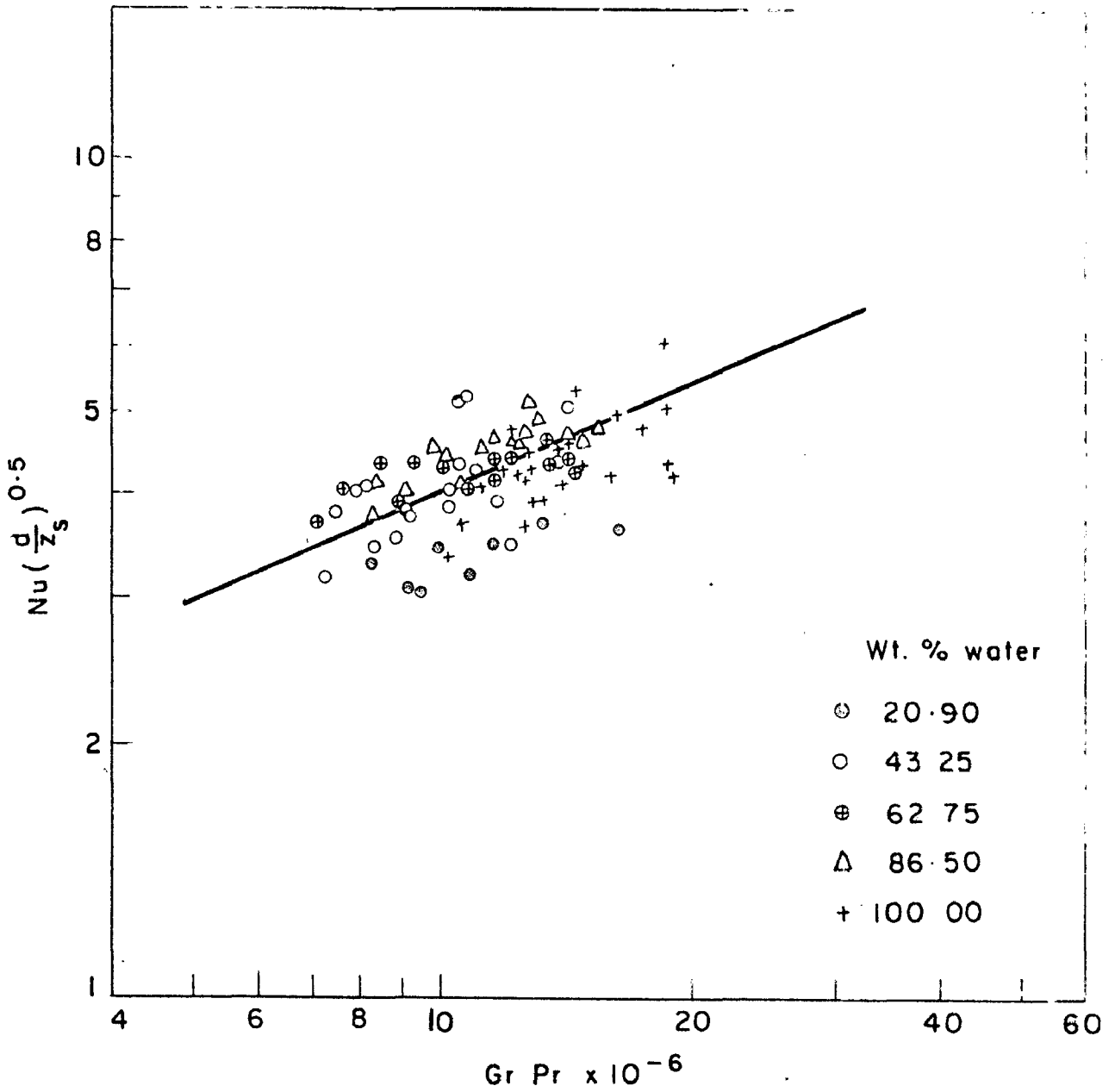
Fig. 4·12 Variation of $Nu(\frac{d}{z_s})^{0.5}$ as a function of $Gr\,Pr$.
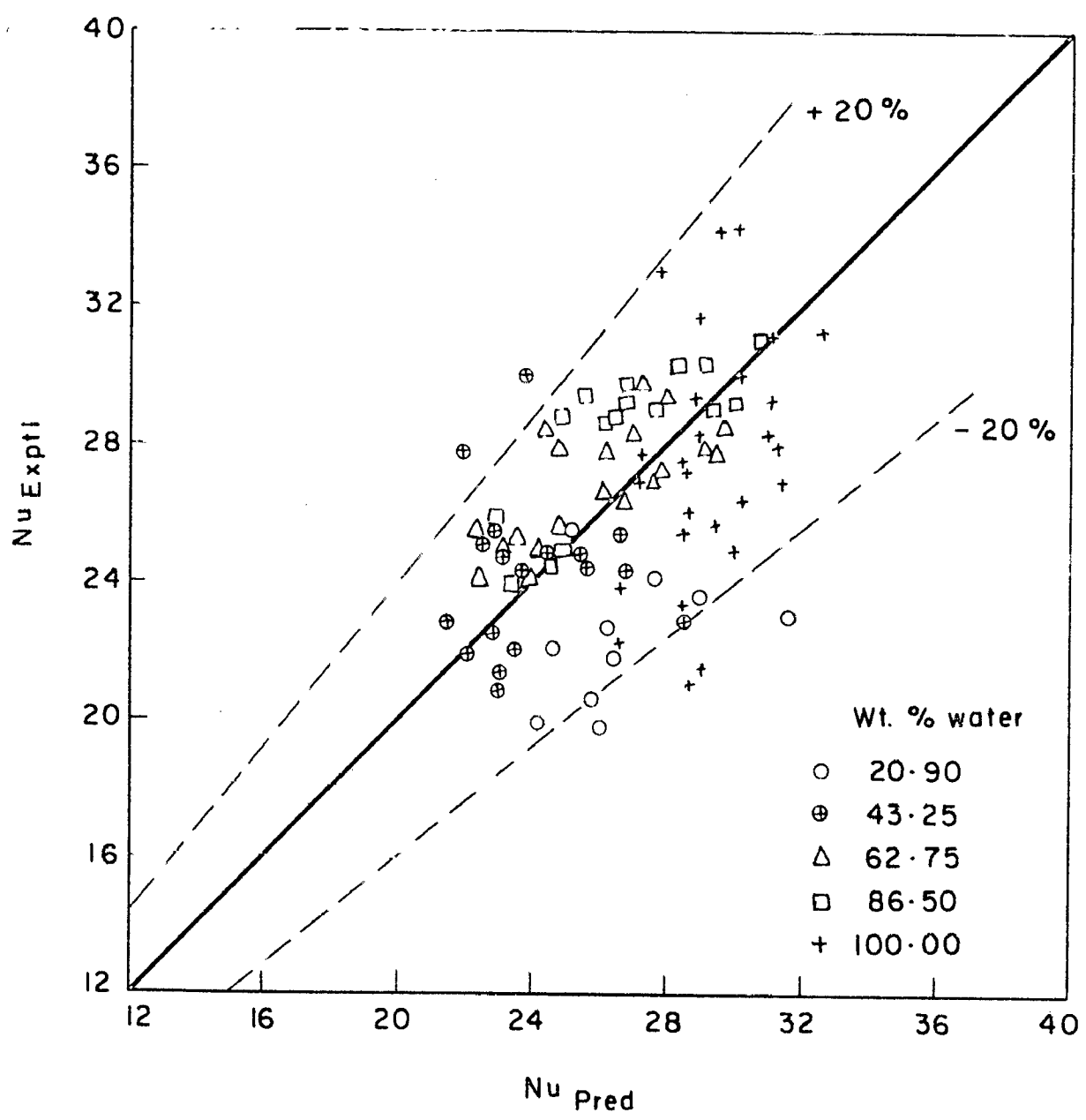
Fig. 4·13 Comparison between the experimental Nusselt numbers and those predicted by eq. (4·2)

A ratio of the velocity of vaporization at the heating surface and the velocity of liquid flowing through the tube as suggested by earlier workers [19,20] for forced convection boiling of subcooled liquids in horizontal tubes was chosen in the following form :

$$\frac{h_B}{h_c} = C_2 \left(\frac{q}{\rho_v \, \lambda \, v}\right)^{n_2} \qquad (4.3)$$

The velocity v in the Eq.(4.3) may be computed by heat balance as under

$$v = \frac{\pi \, d \, z_s \, q}{\frac{\pi \, d^2}{4} \, \rho_L \, C \, (t_s - t_{L_i})} = \frac{4 \, z_s q}{d \, \rho_L \, C \, \Delta t_{sub}} \qquad (4.4)$$

Substituting the value of v from Eq. (4.4) the Eq. (4.3) becomes

$$\frac{h_B}{h_c} = \frac{C_2}{4} \left(\frac{\rho_L}{\rho_v} \, \frac{C}{\lambda} \, \frac{d}{z_s} \, \Delta t_{sub}\right)^{n_2} \qquad (4.5)$$

Figure 4.14 shows a log-log plot of h_B/h_c versus $\frac{\rho_L}{\rho_v} \, \frac{C}{\lambda} \, \frac{d}{z_s} \, \Delta t_{sub}$ for water at $z = z_s$. The average straight line passing through the data points gives the value of exponent $n_2 = -0.33$.

The local values of h_B/h_c vary along the tube length (Figs. 4.5 and 4.11) and seem to depend upon, the

$q \times 10^{-3}, W/m^2$

+	10·66
o	12·44
⊕	14·22
o	15·99
△	17·77
×	19·55
□	21·33
▽	24·88

$\dfrac{h_B}{h_c}\left(\dfrac{\rho_L}{\rho_V}\dfrac{C}{\lambda}\dfrac{d}{z_s}\,\Delta t_{sub}\right)^{0.33}$

$\dfrac{t_L}{t_W}\dfrac{z}{d}$

Fig 4 15 Plot of $\dfrac{h_B}{h_c}\left(\dfrac{\rho_L}{\rho_V}\dfrac{C}{\lambda}\dfrac{d}{z_s}\,\Delta t_{sub}\right)^{0.33}$ vs

$\dfrac{t_L}{t_W}\dfrac{z}{d}$ for water

$z = z_s$

$q \times 10^{-3}, W/m^2$

+	10·66
o	12·44
⊕	15·99
△	17·77
×	19·55
□	21·33
▽	24·88
o	14·22
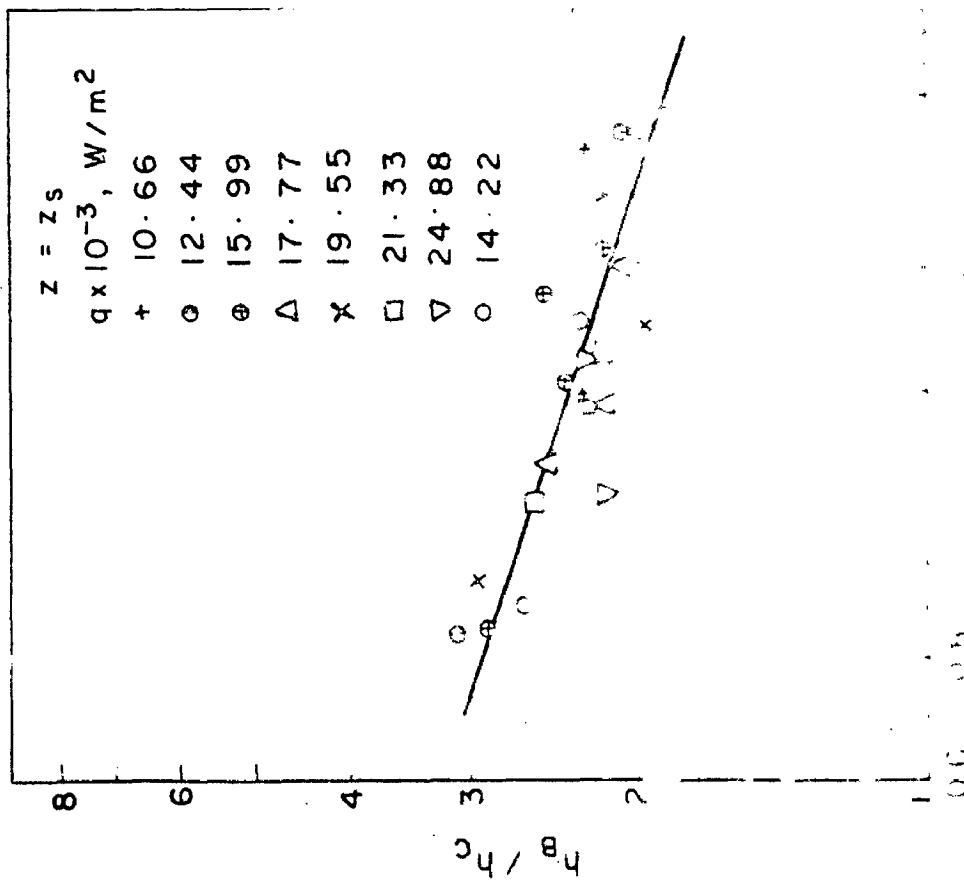
h_B / h_c

$\left(\dfrac{\rho_L}{\rho_V}\dfrac{C}{\lambda}\dfrac{d}{z_s}\,\Delta t_{sub}\right)$

Fig 4 14 Plot of $\dfrac{h_B}{h_c}$ vs $\left(\dfrac{\rho_L}{\rho_V}\dfrac{C}{\lambda}\dfrac{d}{z_s}\,\Delta t_{sub}\right)$
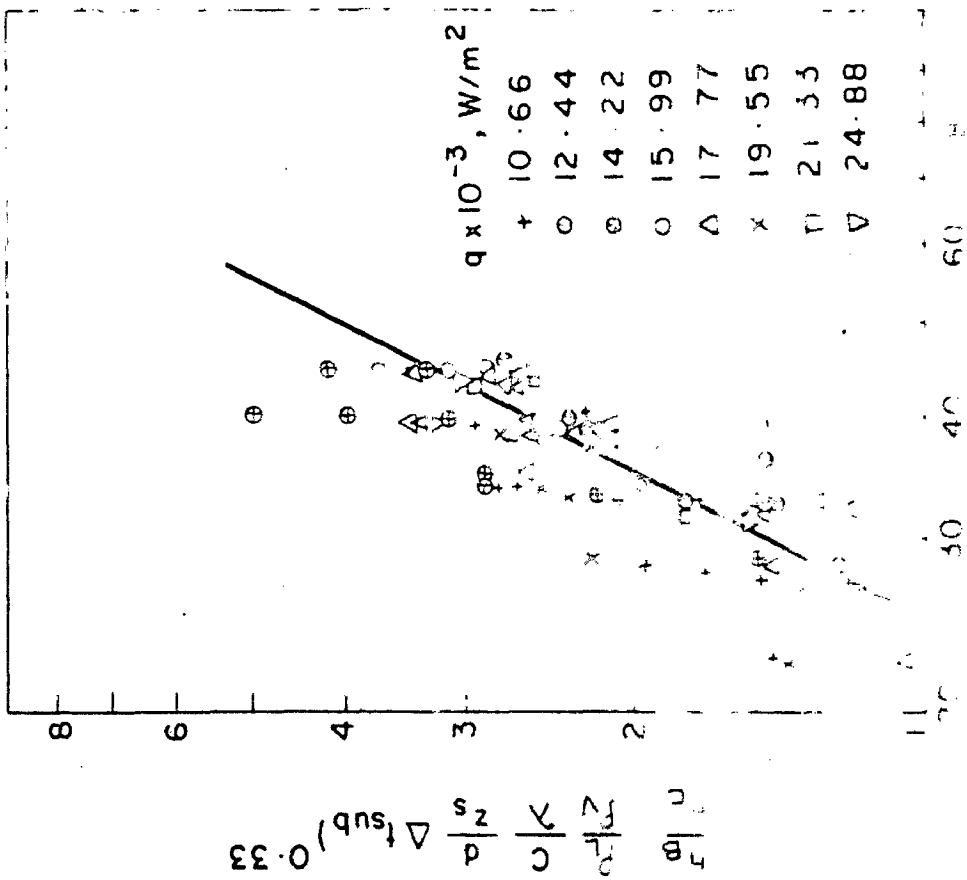
for water

local values of either degree of subcooling or vapour fraction and wall temperature in addition to the subcooling of inlet liquid. In order to account for these parameters conveniently a dimensionless group $\left(\dfrac{t_L}{t_W} \cdot \dfrac{z}{d}\right)$ was chosen. A plot of $\dfrac{h_B}{h_c}\left(\dfrac{\rho_L}{\rho_V} \cdot \dfrac{C}{\lambda} \cdot \dfrac{d}{z_s}\Delta t_{sub}\right)^{0.33}$ versus

$\left(\dfrac{t_L}{t_W} \cdot \dfrac{z}{d}\right)$ for all the data points of water was represented by a straight line having a slope of 2. The final correlation for water thus obtained is

$$\frac{h_B}{h_c} = 1.62 \times 10^{-3} \left(\frac{\rho_L}{\rho_V} \cdot \frac{C}{\lambda} \cdot \frac{d}{z_s}\Delta t_{sub}\right)^{-0.33} \left(\frac{t_L}{t_W} \cdot \frac{z}{d}\right)^2$$

(4.6)

The values of h_B predicted using Eq.(4.6) in conjunction with Eq. (4.2) were compared with the experimentally determined values on a plot as shown in Figure 4.16. A good agreement with a maximum deviation of about $\pm$ 40 per cent is observed for all the data points covering surface as well as bulk boiling of water.

4.3.3 Correlation of Heat Transfer for Natural Circulation Boiling of Water-Glycerine Mixtures in a Vertical Tube

The experimental transfer coefficients for water - glycerine mixtures, were correlated in terms of the same dimensionless groups as obtained for water in the following functional form :
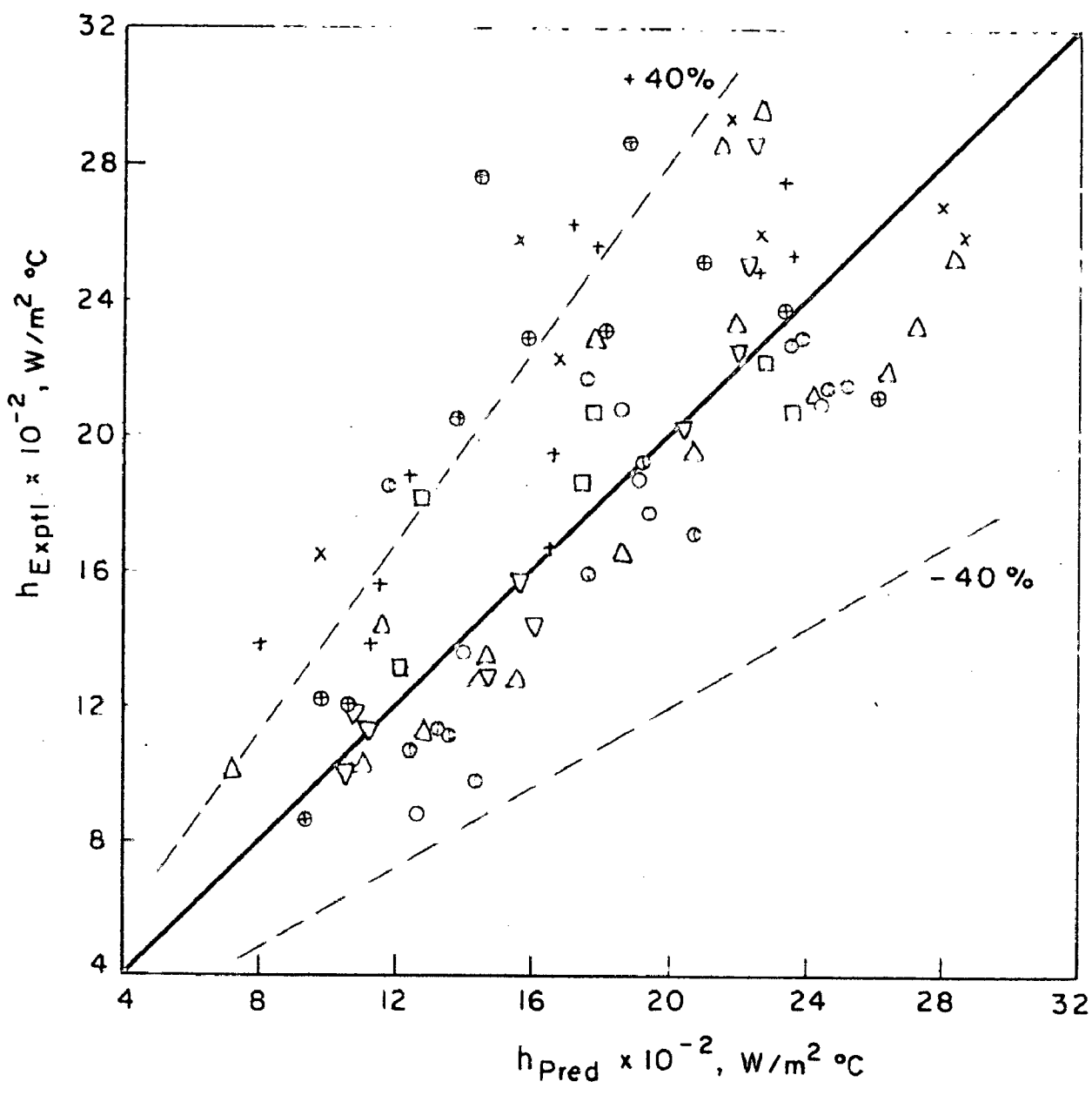
Fig. 4·16   Comparison between the experimental boiling heat transfer coefficient and that predicted by eq. (4·6) for water

$$\frac{h_B}{h_c} = C_3 \left(\frac{\rho_L}{\rho_V} \cdot \frac{C}{\lambda} \cdot \frac{d}{z_s} \Delta t_{sub}\right)^{n_3} \left(\frac{t_L}{t_W} \cdot \frac{z}{d}\right)^m \qquad (4.7)$$

Figures 4.17 to 4.20 show the plots of h_B/h_c versus $\left(\frac{\rho_L}{\rho_V} \cdot \frac{C}{\lambda} \cdot \frac{d}{z_s} \Delta t_{sub}\right)$ at $z = 900$ mm for various

compositions of water glycerine mixtures. The slopes of the straight lines representing the data points yield the values of exponent n_3. Using these corresponding values of exponents, plots of $\frac{h_B}{h_c} \left(\frac{\rho_L}{\rho_V} \cdot \frac{C}{\lambda} \cdot \frac{d}{z_s} \Delta t_{sub}\right)^{-n_3}$ versus

$\left(\frac{t_L}{t_W} \cdot \frac{z}{d}\right)$ were made as shown in Figures 4.21 to 4.24.

The slope of all the straight lines representing data for various compositions of the mixture was found to be 2.3. However, the values of constant C_3 in Eq. (4.7) was found to depend upon the composition. The values of exponents n_3 and m and constant C_3 are presented in Table 4.2 .

Table 4.2 Values of Exponents and constants in Eq.(4.7)

Mixture composition wt.% water	n_3	m	$c \times 10^4$
20.9	1.00	2.3	5.28
43.25	0.185	2.3	6.52
62.75	0.12	2.3	5.42
85.5	0.045	2.3	4.57
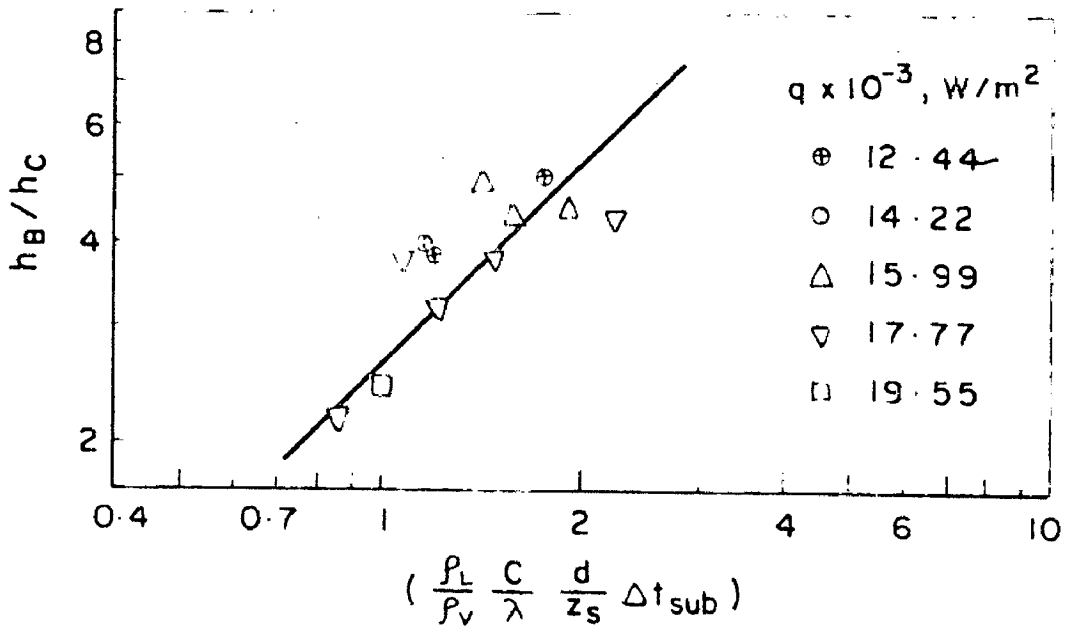
Fig. 4·17 Plot of $\dfrac{h_B}{h_c}$ vs $\left(\dfrac{\rho_L}{\rho_v} \dfrac{C}{\lambda} \dfrac{d}{z_s} \Delta t_{sub}\right)$ for 20·90 wt. % water
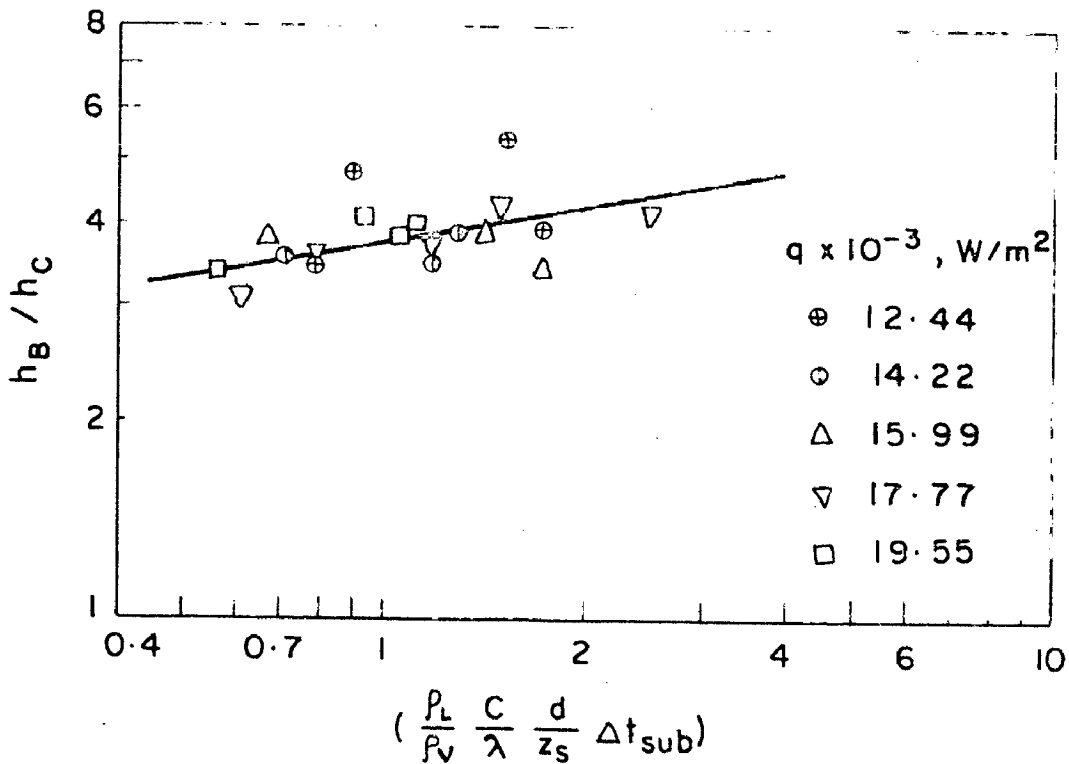
Fig. 4·18 Plot of $\dfrac{h_B}{h_c}$ vs $\left(\dfrac{\rho_L}{\rho_v} \dfrac{C}{\lambda} \dfrac{d}{z_s} \Delta t_{sub}\right)$ for 43·25 wt % water
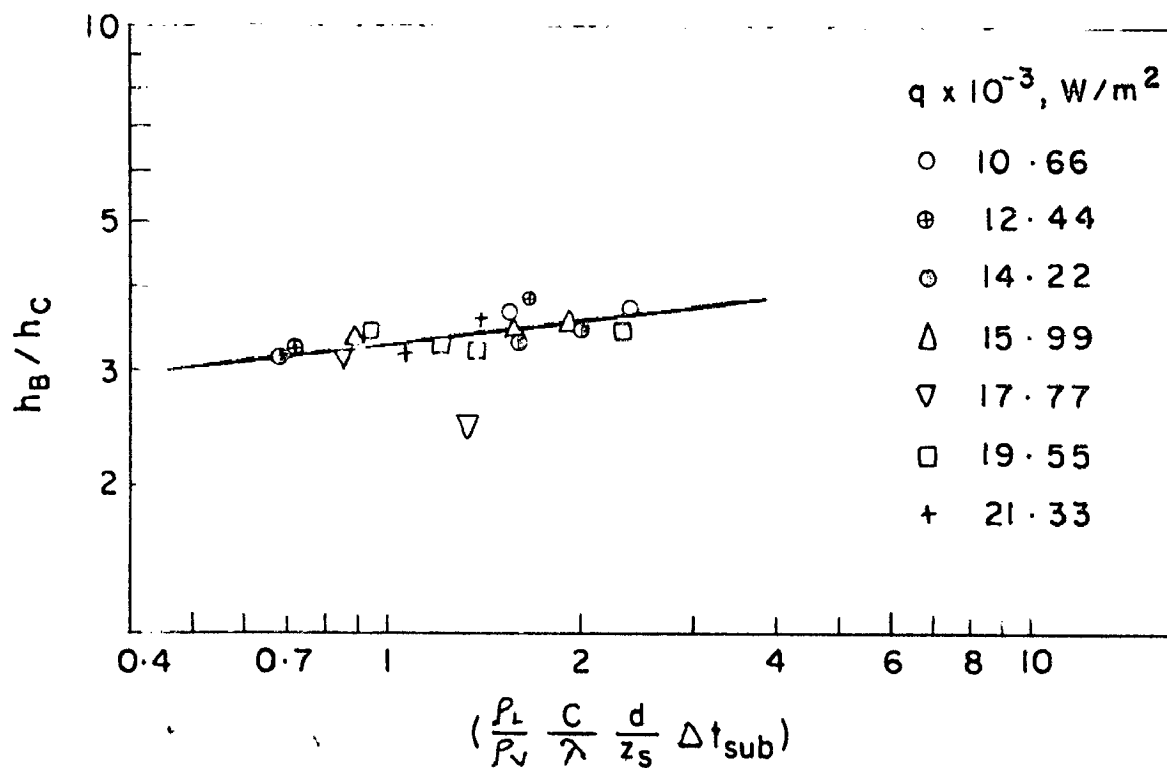
Fig. 4·19 Plot of $\frac{h_B}{h_C}$ vs $\left(\frac{\rho_L}{\rho_V} \frac{C}{\lambda} \frac{d}{z_s} \Delta t_{sub}\right)$ for 62·75 wt. % water
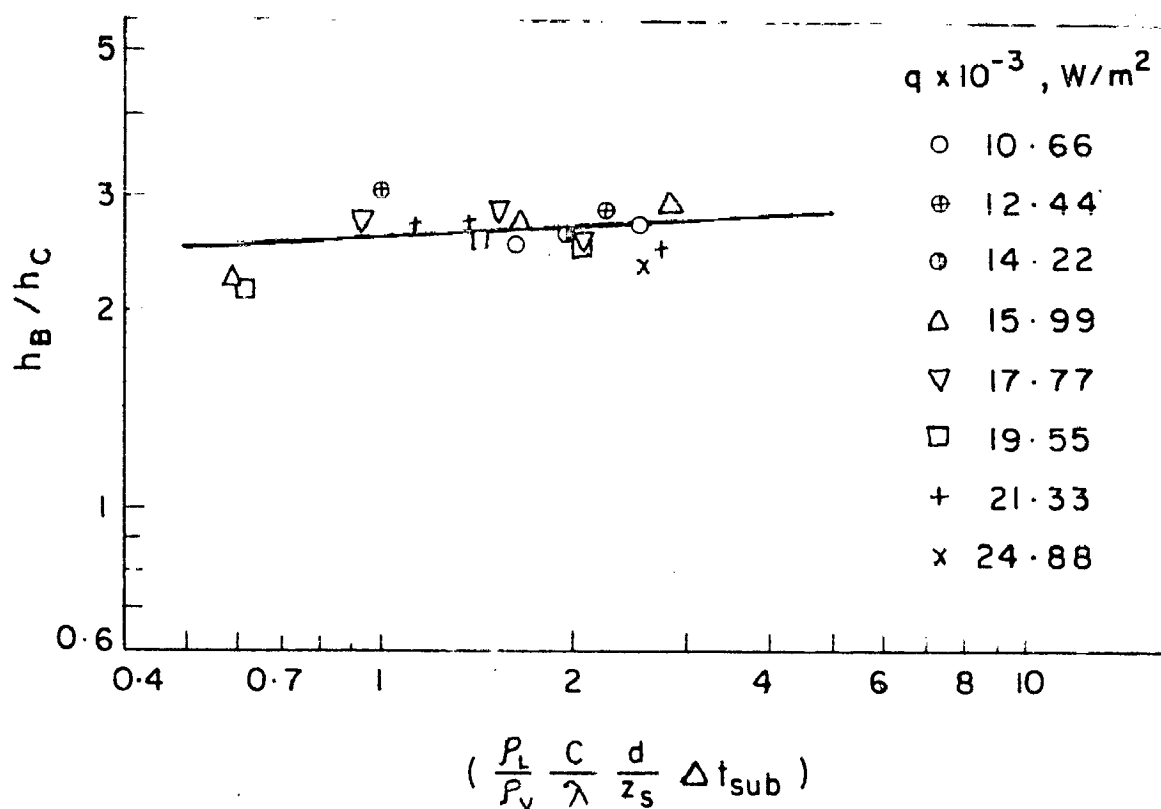
Fig. 4·20 Plot of $\frac{h_B}{h_C}$ vs $\left(\frac{\rho_L}{\rho_V} \frac{C}{\lambda} \frac{d}{z_s} \Delta t_{sub}\right)$ for 86·50 wt. % water

Fig. 4.22 Plot of $\dfrac{h_B}{h_C}\left(\dfrac{\rho_L}{\rho_V}\dfrac{C}{\lambda}\dfrac{d}{z_s}\Delta t_{sub}\right)^{-0.185}$

vs $\dfrac{t_L}{t_W}\dfrac{z}{d}$ for 43.25 wt. % water
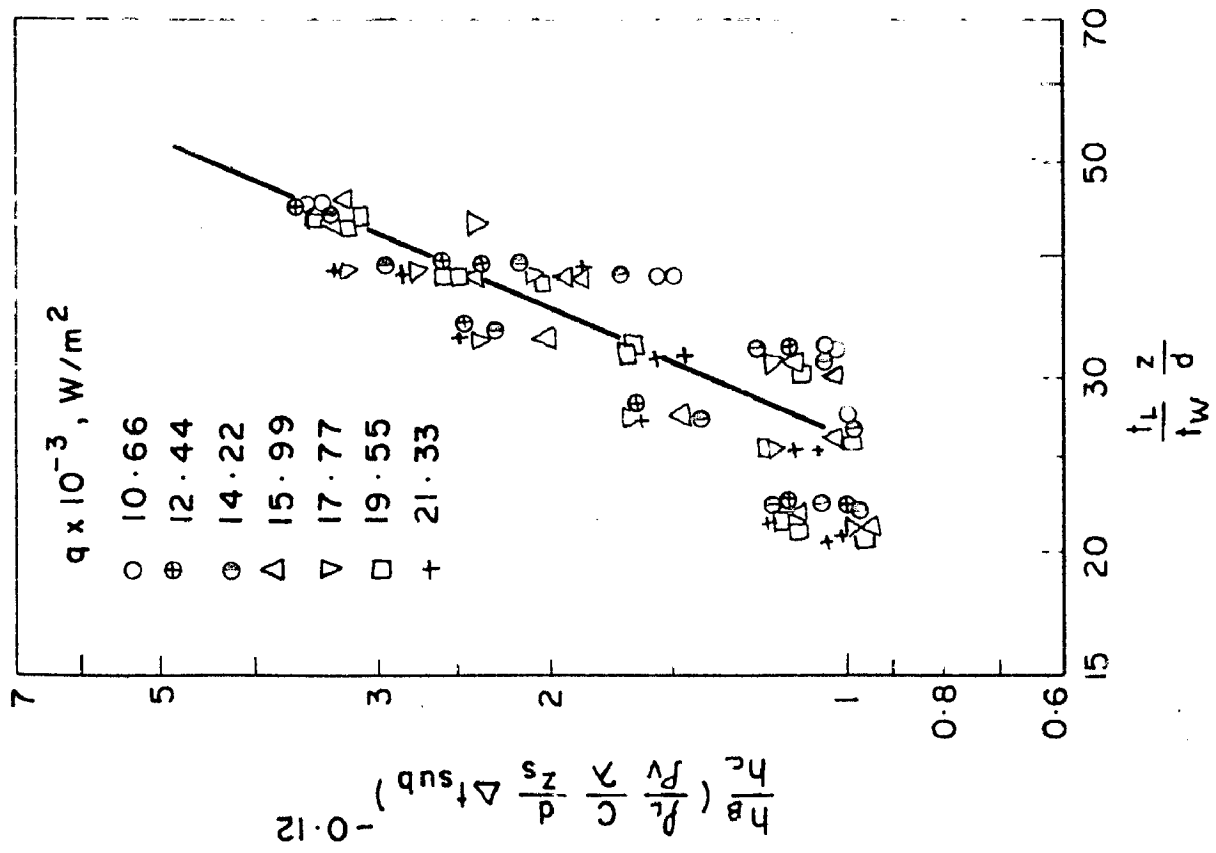
Fig. 4.21 Plot of $\dfrac{h_B}{h_C}\left(\dfrac{\rho_L}{\rho_V}\dfrac{C}{\lambda}\dfrac{d}{z_s}\Delta t_{sub}\right)^{-1}$ vs $\dfrac{t_L}{t_W}\dfrac{z}{d}$

for 20.9 wt. % water

Fig. 4.24 Plot of $\dfrac{h_B}{h_c}\left(\dfrac{f_L}{P_V}\dfrac{C}{\lambda}\dfrac{d}{z_s}\Delta t_{sub}\right)^{-0.045}$
vs $\dfrac{t_L}{t_w}\dfrac{z}{d}$ for 86·50 wt. % water

Fig. 4.23 Plot of $\dfrac{h_B}{h_c}\left(\dfrac{f_L}{P_V}\dfrac{C}{\lambda}\dfrac{d}{z_s}\Delta t_{sub}\right)^{-0.12}$ vs
$\dfrac{t_L}{t_w}\dfrac{z}{d}$ for 62·75 wt. % water
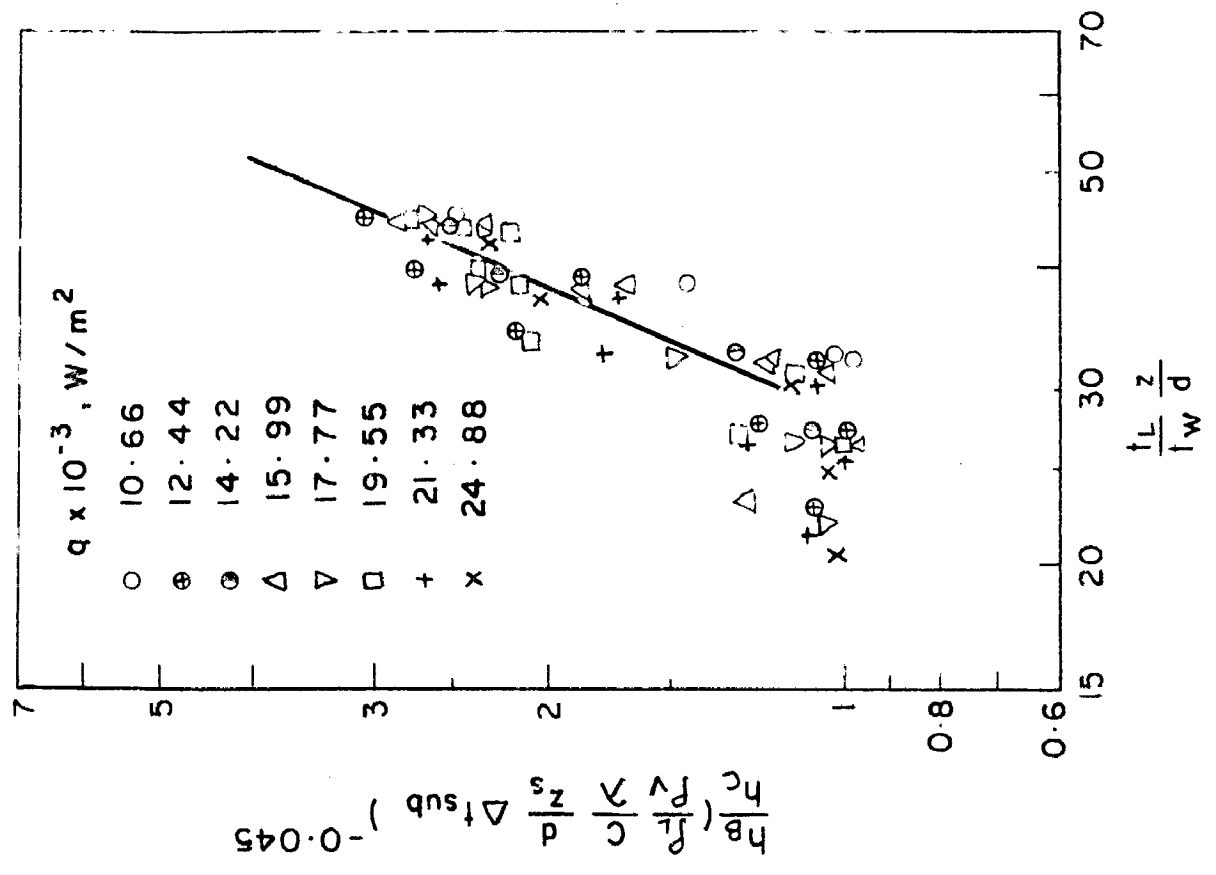
Figure 4.25 shows a comparison between the
experimental values of h_B and those predicted by
Eq. (4.7) using respective values of exponents and
constants. Almost all the data points of surface and
saturated boiling agree well with a maximum deviation of
$\pm$ 40 per cent.
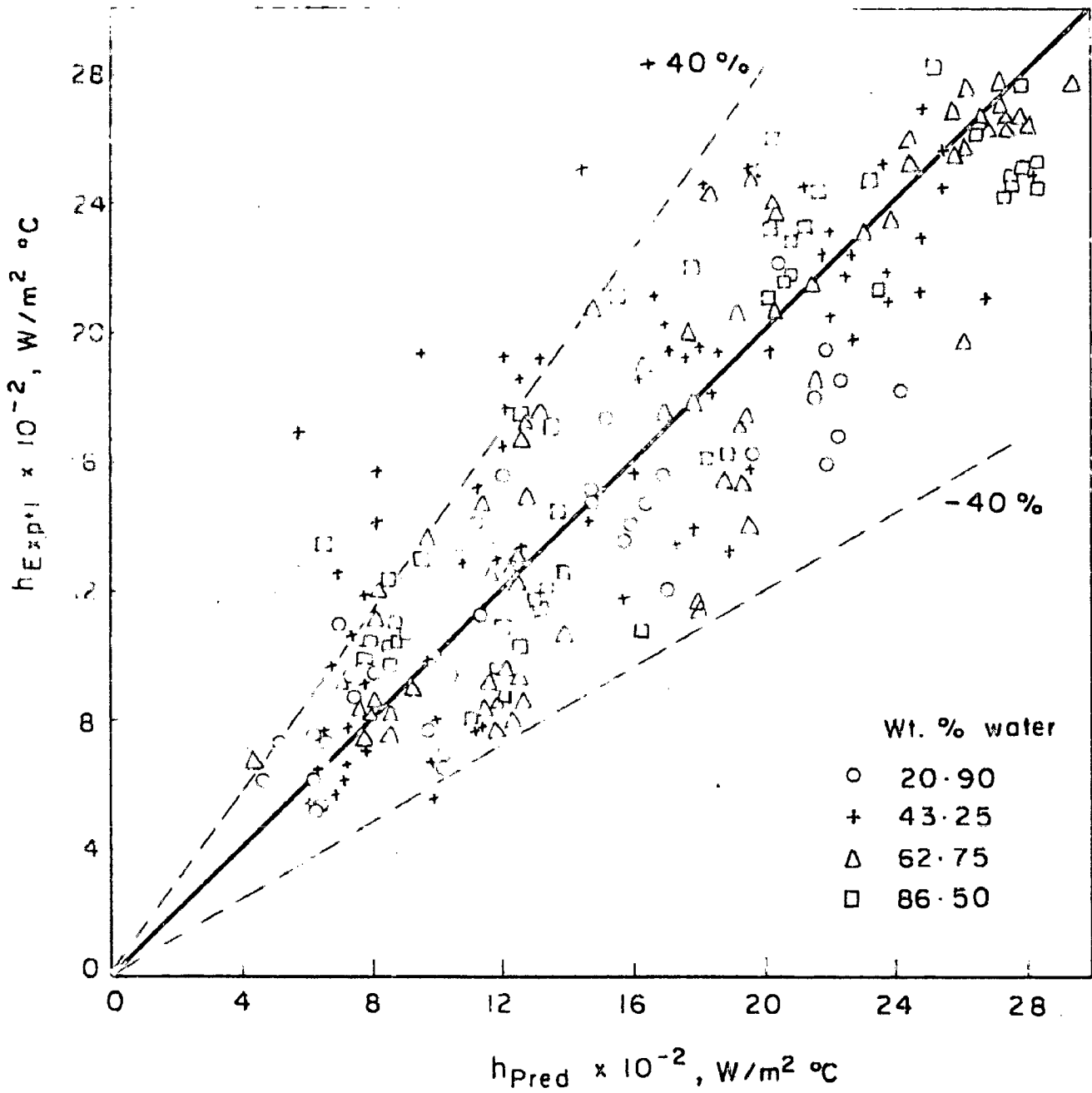
Fig. 4·25 Comparison between experimental boiling heat transfer
coefficient and that predicted by eq. (4·7) for water-
glycerine mixtures

C H A P T E R 5

CONCLUSIONS AND RECOMMENDATIONS

1.   The wall and liquid temperature distributions at uniform heat flux over the entire tube length have shown the existence of three distinct regions of heat transfer namely single phase natural convection, subcooled boiling and saturated boiling with appearance of vapor phase, along the tube length if a subcooled liquid enters the heated tube.

2.   The heat transfer coefficient in natural convective region was observed to remain almost constant whereas it increased sharply in surface boiling along the tube length. The values of transfer coefficients increased with rise in q. The degree of subcooling of inlet liquid was found to affect the heat transfer coefficient during boiling significantly; the values of h being higher at lower values of Δt_{sub}.

3.   The heat transfer coefficients for water-glycerine mixtures increased with increase in water concentration in all the three regions. However, the rise in values during natural convection was relatively higher than that in boiling.

4.   Experimental data of single phase natural convective region for water and four water-glycerine mixtures were

correlated by the following equation with a maximum error of $\pm$ 20 per cent.

$$Nu = 3.33 \times 10^{-3} (Gr\ Pr)^{0.44} \left(\frac{z_s}{d}\right)^{0.5}$$

The range of $Gr\ Pr$ covered was 7.11×10^6 - 19.0×10^6.

5. A correlation for calculating heat transfer coefficient during subcooled and saturated boiling of liquids investigated, is recommended in the following general form :

$$\frac{h_B}{h_c} = C_3 \left(\frac{\rho_L}{\rho_V} \cdot \frac{c}{\lambda} \cdot \frac{d}{z_s}\Delta t_{sub}\right)^{n_3} \left(\frac{t_L}{t_w} \cdot \frac{z}{d}\right)^m$$

The values of C_3, n_3 and m were found to be 1.62×10^{-3}, -0.33 and 2 respectively for water. For water-glycerine mixtures, the values are given in Table 4.2. The maximum deviation of all the experimental data points in subcooled as well as saturated boiling regions was about $\pm$ 40 per cent.

From the results of the present investigation, the following recommendations for future study are made:

1. The correlation for single phase natural convective heat transfer was obtained based only on water and water-glycerine solutions and as such is applicable over a narrow range of parameters studied. The study may be

extended to other systems with different tube diameters
and lengths.

2. The investigation on boiling of pure liquids may
be extended to more liquids, having widely varying physi-
cal properties, using high heat fluxes, and wide range
of operating parameters. The effect of tube diameter
and length with different submergences should be inclu-
ded in the study.

3. The boiling of liquid mixtures and aqueous salt
solutions will not only yield interesting results but
will also be of great practical importance.

The analytical approach to the above should form
the basis of generalized correlations to represent the exp-
erimental data points.

APPENDIX   A

TABLES   OF   CALIBRATION

Table A.1   PERFORMANCE OF THERMOCOUPLES

Standard Thermometer °C		Inlet Thermocouple	WALL THERMOCOUPLES $z \times 10^{-2}$										Outlet Thermocouple
			0	1	2	3	4	5	6	7	8	9	
60.50	mv	2.470	2.468	2.466	2.471	2.466	2.468	2.466	2.470	2.470	2.469	2.471	2.466
	°C	60.50	60.45	60.40	60.50	60.40	60.45	60.40	60.50	60.50	60.45	60.50	60.40
76.30	mv	3.166	3.164	3.168	3.164	3.168	3.165	3.166	3.168	3.164	3.167	3.166	3.164
	°C	76.35	76.30	76.40	76.30	76.40	76.35	76.35	76.40	76.30	76.40	76.35	76.30
95.0	mv	4.012	4.009	4.007	4.011	4.010	4.010	4.010	4.012	4.011	4.010	4.014	4.009
	°C	95.05	95.00	94.95	95.05	95.00	95.00	95.00	95.05	95.05	95.00	95.10	95.00
106.4	mv	4.536	4.536	4.535	4.538	4.536	4.533	4.533	4.535	4.536	4.536	4.533	4.533
	°C	106.40	106.40	106.40	106.45	106.40	106.35	106.35	106.40	106.40	106.40	106.35	106.35

Table A.2   CALIBRATION   OF   WATTMETER

Wattmeter readings, W		Error %
Substandard	Wattmeter	
640	650	+ 1.54
960	950	- 1.05
1200	1180	- 1.69
1340	1320	- 1.51
1485	1470	- 1.02

Table A.3   CALIBRATION OF FLOWMETER FOR WATER

Manometer reading cm.	Flow rate Litre/min	Manometer reading cm.	Flow rate Litre/min
0.75	1.191	9.35	3.425
1.05	1.358	11.30	3.790
1.55	1.582	13.20	4.080
2.05	1.593	15.25	4.375
2.70	2.000	17.25	4.645
3.50	2.095	19.25	4.880
4.45	2.345	20.95	5.155
5.45	2.640	24.45	5.610
7.40	3.035	27.50	5.960

Table A. 4   HEAT BALANCE

Energy input W	500	700	900	1100
Heat flux W/m^2	8.88×10^3	12.44×10^3	15.99×10^3	19.55×10^3
Flow rate Kg/hr	107.2	106.5	105.7	106.8
$z \times 10^{-2}$ mm	Wall temperature , ^0C			
0	26.13	27.45	29.46	30.68
1	33.77	37.32	41.39	44.78
2	37.49	42.38	46.95	50.88
3	40.20	45.61	50.83	55.23
4	44.21	50.50	56.96	61.68
5	44.05	50.64	56.33	61.53
6	46.33	53.60	59.73	65.41
7	47.65	54.84	60.83	66.58
8	50.40	58.53	65.03	71.69
9	51.87	60.10	67.08	73.61
Inlet temperature ^0C	23.18	23.35	24.20	24.43
Outlet temperature ^0C	27.17	28.95	31.41	33.17
Heat loss %	0.47	0.83	1.55	1.38
Experimental Average h $W/m^2 \ ^0C$	451	490	540	579
Predicted h $W/m^2 \ ^0C$	465	522	485	566
Deviation %	-3.01	-6.13	+11.35	+2.30

APPENDIX   B

EXPERIMENTAL   DATA

Table B.1   Experimental Data of Heat Transfer
to Water.

Table B.2   Experimental Data of Heat Transfer
to Water-Glycerine Mixtures.

Table B.1 EXPERIMENTAL DATA OF HEAT TRANSFER TO WATER

$z \times 10^{-2}$ mm	Temperature, °C		h W/m2 °C	$z \times 10^{-2}$ mm	Temperature, °C		h W/m2 °C
	t_W	t_L			t_W	t_L	

$q = 10.66 \times 10^3$ W/m^2

Run No. 1   **Run No. 4**

$z \times 10^{-2}$ mm	t_W	t_L	h W/m2 °C	$z \times 10^{-2}$ mm	t_W	t_L	h W/m2 °C
0	81.55	77.45	2600	0	84.87	78.55	1970
1	91.62	80.10	926	1	95.60	81.20	864
2	94.95	82.75	874	2	97.28	83.80	923
3	97.38	85.50	898	3	101.32	86.50	840
4	102.53	88.20	744	4	105.98	89.00	733
5	103.70	90.80	827	5	107.55	91.60	780
6	106.56	93.60	823	6	108.49	94.20	871
7	108.30	96.25	885	7	102.95	96.90	2056
8	104.70	99.00	1870	8	103.34	99.00	2868
9	104.08	99.00	2100	9	104.25	99.00	2370

Run No. 2   **Run No. 5**

$z \times 10^{-2}$ mm	t_W	t_L	h W/m2 °C	$z \times 10^{-2}$ mm	t_W	t_L	h W/m2 °C
0	67.02	61.57	1953	0	72.60	66.02	1890
1	78.40	66.00	860	1	84.43	70.30	881
2	84.10	70.50	784	2	89.56	74.50	826
3	87.90	75.00	826	3	94.80	78.50	763
4	94.80	79.60	702	4	100.52	82.50	690
5	97.65	84.10	787	5	103.02	86.60	757
6	102.48	88.70	774	6	108.70	90.65	689
7	107.60	93.20	768	7	105.00	94.80	1220
8	105.53	97.70	1362	8	103.50	99.00	2765
9	104.12	99.00	2083	9	104.38	99.00	2312

$q = 12.44 \times 10^3$ W/m^2 $q = 14.22 \times 10^3$ W/m^2

Run No. 3   **Run No. 6**

$z \times 10^{-2}$ mm	t_W	t_L	h W/m2 °C	$z \times 10^{-2}$ mm	t_W	t_L	h W/m2 °C
0	94.80	88.00	1830	0	97.00	94.80	6460
1	104.12	89.40	846	1	105.70	95.50	1394
2	107.15	90.90	766	2	110.83	96.30	978
3	106.90	92.30	852	3	110.28	97.10	1080
4	114.17	93.75	609	4	110.60	97.90	1120
5	112.02	95.10	734	5	108.50	98.60	1436
6	106.87	96.60	1210	6	106.50	99.00	1895
7	103.55	98.10	2283	7	106.05	99.00	2018
8	103.95	99.00	2512	8	105.63	99.00	2145
9	104.85	99.00	2126	9	105.63	99.00	2145

$z \times 10^{-2}$ mm	Temperature, °C		$\dfrac{h}{W/m^2 \, °C}$	$z \times 10^{-2}$ mm	Temperature, °C		$\dfrac{h}{W/m^2 \, °C}$
	t_W	t_L			t_W	t_L	

Run No.7

				Run No.10			
0	94.80	87.70	2002	0	78.86	72.60	2270
1	101.33	89.10	1163	1	90.20	75.90	994
2	107.00	90.70	972	2	94.80	79.10	905
3	107.75	92.30	920	3	97.00	82.30	967
4	111.13	94.00	830	4	102.30	85.50	846
5	110.53	95.60	953	5	103.98	88.60	925
6	109.70	97.20	1137	6	107.05	91.80	933
7	106.60	98.90	1846	7	108.40	95.05	1065
8	105.55	99.00	2170	8	107.21	98.30	1595
9	105.25	99.00	2275	9	105.21	99.00	2290

Run No.8

				Run No.11			
0	80.85	76.00	2930	0	61.68	55.37	2252
1	94.80	79.00	900	1	75.43	60.40	946
2	97.00	82.00	948	2	81.58	65.25	871
3	99.17	85.00	1003	3	84.54	70.15	988
4	105.04	88.00	835	4	92.15	75.00	829
5	105.63	91.00	972	5	94.80	79.90	955
6	109.21	94.10	941	6	99.22	84.90	993
7	109.75	97.20	1133	7	103.70	89.90	1030
8	106.43	99.00	1914	8	109.15	94.70	983
9	105.63	99.00	2145	9	107.32	99.00	1710

$$q = 15.99 \times 10^3 \quad W/m^2$$

Run No.9

				Run No.12			
0	77.82	73.41	3225	0	94.80	88.45	2520
1	89.74	76.70	1090	1	101.70	90.00	1366
2	95.34	80.00	927	2	107.17	91.50	1020
3	97.00	83.40	1045	3	109.92	93.00	945
4	102.83	86.80	987	4	113.88	94.50	825
5	104.33	90.00	993	5	111.77	96.00	1014
6	108.10	93.50	973	6	108.58	97.40	1430
7	109.53	96.80	1118	7	105.98	99.00	2290
8	107.00	99.00	1778	8	104.40	99.00	2962
9	105.63	99.00	2145	9	105.33	99.00	2525

$z \times 10^{-2}$ mm	Temperature, °C t_W	t_L	h W/m² °C	$z \times 10^{-2}$ mm	Temperature, °C t_W	t_L	h W/m² °C

Run No.13

				Run No.16			
0	84.05	78.64	2956	0	65.77	58.40	2170
1	95.32	81.30	1141	1	79.35	63.00	978
2	101.33	84.00	921	2	84.15	67.75	975
3	101.65	86.65	1066	3	88.24	72.50	1015
4	107.36	89.25	883	4	94.80	77.10	903
5	108.27	91.85	973	5	98.20	81.80	975
6	110.68	94.50	988	6	102.75	86.50	984
7	109.47	97.00	1288	7	106.75	91.25	1031
8	104.60	99.00	2856	8	108.50	96.00	1280
9	106.28	99.00	2197	9	105.87	99.00	2330

$$q = 17.77 \times 10^3 \quad W/m^2$$

Run No.14

				Run No.17			
0	76.85	72.60	3763	0	87.71	82.02	3125
1	89.58	75.80	1160	1	98.65	84.20	1230
2	94.80	79.15	1022	2	104.20	86.30	992
3	97.00	82.50	1102	3	106.67	88.45	975
4	102.96	85.75	929	4	109.92	90.60	920
5	103.50	89.00	1102	5	109.92	92.80	1038
6	107.40	92.30	1059	6	109.92	95.00	1190
7	107.55	95.70	1350	7	108.55	97.20	1570
8	107.21	99.00	1957	8	105.21	99.00	2863
9	105.85	99.00	2335	9	107.79	99.00	2022

Run No.15

				Run No.18			
0	74.52	69.10	2950	0	81.58	78.60	5960
1	87.70	72.70	1066	1	94.80	81.00	1288
2	92.18	76.20	1000	2	100.30	83.50	1058
3	94.80	79.80	1066	3	101.90	86.00	1117
4	101.06	83.30	900	4	105.64	88.50	1036
5	102.60	86.80	1012	5	107.80	91.00	1057
6	106.06	90.50	1026	6	109.17	93.50	1134
7	108.23	94.00	1124	7	108.24	96.00	1453
8	107.23	97.60	1660	8	105.70	98.60	2505
9	106.60	99.00	2103	9	107.27	99.00	2150

$z \times 10^{-2}$ mm	Temperature, °C		h W/m² °C	$z \times 10^{-2}$ mm	Temperature, °C		h W/m² °C
	t_W	t_L			t_W	t_L	

Run No.19

0	74.86	70.34	3932
1	88.24	73.75	1226
2	94.80	77.20	1010
3	94.80	80.60	1251
4	101.33	84.00	1025
5	102.27	87.50	1203
6	106.40	91.00	1155
7	108.30	94.40	1280
8	105.63	97.75	2255
9	107.80	99.00	2020

Run No.22

0	85.40	79.13	3120
1	98.87	82.25	1176
2	103.82	85.25	1153
3	104.33	88.25	1215
4	109.60	91.25	1165
5	109.92	94.25	1247
6	108.00	97.25	1820
7	108.47	99.00	2065
8	108.38	99.00	2085
9	108.38	99.00	2085

Run No.20

0	66.79	58.87	2245
1	81.17	63.55	1010
2	86.92	68.20	950
3	92.63	72.90	901
4	98.15	77.50	861
5	100.78	82.15	954
6	104.60	86.85	1001
7	107.84	91.50	1008
8	109.92	96.15	1290
9	107.80	99.00	2020

$$q = 19.55 \times 10^3 \ \text{W/m}^2$$

Run No.23

0	72.60	65.77	2862
1	88.09	69.75	1066
2	94.80	73.80	931
3	95.82	77.80	1085
4	103.50	81.80	901
5	104.63	85.90	1044
6	108.49	90.00	1057
7	108.93	94.00	1310
8	108.57	98.10	1867
9	107.80	99.00	2220

$$q = 21.33 \times 10^3 \ \text{W/m}^2$$

Run No.21

0	94.80	88.70	3205
1	104.95	90.25	1330
2	113.20	92.00	922
3	116.30	93.60	861
4	110.80	95.30	1261
5	107.60	97.00	1844
6	107.36	98.65	2245
7	105.91	99.00	2830
8	103.71	99.00	4100
9	107.25	99.00	2370

Run No.24

0	94.80	86.25	2495
1	102.66	88.15	1470
2	109.08	90.10	1114
3	114.17	92.00	962
4	116.30	94.00	957
5	110.06	96.00	1516
6	108.87	98.00	1961
7	106.96	99.00	2680
8	107.21	99.00	2600
9	108.16	99.00	2330

$z \times 10^{-2}$ mm	Temperature, °C		h	$z \times 10^{-2}$ mm	Temperature, °C		h
	t_W	t_L	W/m² °C		t_W	t_L	W/m² °C

$$q = 24.88 \times 10^3 \ \text{W/m}^2$$

Run No.25

				Run No.28			
0	87.52	81.65	3635	0	92.52	86.80	4350
1	99.33	84.00	1391	1	104.12	88.80	1624
2	106.10	86.50	1087	2	111.90	90.80	1180
3	109.35	89.00	1047	3	112.90	92.80	1237
4	112.76	91.50	1003	4	114.58	94.75	1255
5	111.78	94.00	1200	5	111.83	96.75	1650
6	110.06	96.40	1561	6	108.40	98.75	2580
7	107.14	99.00	2620	7	107.48	99.00	2933
8	107.58	99.00	2486	8	108.33	99.00	2670
9	109.48	99.00	2035	9	108.73	99.00	2556

Run No.26

				Run No.29			
0	84.10	78.07	3535	0	85.70	79.00	3712
1	95.86	80.90	1425	1	101.48	81.75	1260
2	102.37	83.65	1140	2	107.27	84.50	1092
3	105.33	86.45	1130	3	108.47	87.20	1170
4	110.98	89.20	980	4	114.80	90.00	1003
5	109.92	92.00	1190	5	113.60	92.70	1190
6	110.13	94.75	1386	6	113.05	95.45	1413
7	108.47	97.50	1944	7	109.38	98.20	2224
8	106.75	99.00	2750	8	108.63	99.00	2585
9	109.02	99.00	2130	9	108.63	99.00	2585

Run No.27

0	76.05	72.60	6180
1	93.68	76.10	1213
2	97.15	79.50	1208
3	99.16	82.85	1307
4	104.55	86.20	1163
5	107.19	89.60	1212
6	109.92	93.00	1260
7	109.06	96.30	1672
8	107.96	99.00	2380
9	108.67	99.00	2206

Table B.2   EXPERIMENTAL DATA OF HEAT TRANSFER TO WATER-GLYCERINE MIXTURES.

$z \times 10^{-2}$ mm	Temperature, °C		h W/m^2 °C		$z \times 10^{-2}$ mm	Temperature, °C		h W/m^2 °C
	t_W	t_L				t_W	t_L	

20.90 wt % WATER
$$q = 12.44 \times 10^3 \ \text{W/m}^2$$

Run No.1

$z \times 10^{-2}$ mm	t_W	t_L	h
0	108.00	95.70	1010
1	126.53	98.65	446
2	134.65	101.65	377
3	137.05	104.60	383
4	138.78	107.60	399
5	137.15	110.65	469
6	133.96	113.70	614
7	131.00	116.70	870
8	126.85	118.00	1405
9	126.25	118.00	1507

Run No.4

$z \times 10^{-2}$ mm	t_W	t_L	h
0	107.55	95.77	1207
1	127.02	98.65	501
2	135.47	101.65	421
3	138.35	104.65	422
4	140.45	107.65	433
5	135.73	110.65	567
6	133.41	113.70	721
7	131.75	116.70	945
8	127.15	118.00	1555
9	126.46	118.00	1680

$$q = 15.99 \times 10^3 \ \text{W/m}^2$$

Run No.2

$z \times 10^{-2}$ mm	t_W	t_L	h
0	95.02	82.00	955
1	114.57	86.50	441
2	123.25	90.85	384
3	127.20	95.20	389
4	131.56	99.60	389
5	131.04	104.10	462
6	131.87	108.50	532
7	130.92	113.00	694
8	125.86	117.40	1470
9	124.40	118.00	1944

Run No.5

$z \times 10^{-2}$ mm	t_W	t_L	h
0	104.16	90.45	1166
1	125.05	93.90	513
2	134.79	97.45	428
3	137.15	101.05	443
4	138.07	104.55	977
5	133.75	108.10	623
6	133.02	111.75	751
7	131.38	115.25	991
8	127.23	118.00	1732
9	125.25	118.00	2205

$$q = 14.22 \times 10^3 \ \text{W/m}^2$$

Run No.3

$z \times 10^{-2}$ mm	t_W	t_L	h
0	110.62	100.00	1340
1	129.57	102.55	526
2	138.96	105.10	420
3	142.87	107.65	404
4	142.82	110.20	436
5	140.20	112.90	521
6	133.72	115.50	780
7	131.77	118.00	1033
8	127.40	118.00	1513
9	126.27	118.00	1720

Run No.6

$z \times 10^{-2}$ mm	t_W	t_L	h
0	99..72	85.70	1140
1	121.50	89.60	501
2	130.74	93.50	429
3	133.02	97.40	449
4	137.15	101.30	446
5	137.15	105.15	500
6	135.20	109.05	611
7	133.75	113.00	770
8	128.70	116.90	1355
9	126.22	118.00	1945

$z \times 10^{-2}$ mm	Temperature, °C t_W	t_L	h W/m² °C	$z \times 10^{-2}$ mm	Temperature, °C t_W	t_L	h W/m² °C

Run No.7   **Run No.10**

0	94.80	77.1?	904	0	110.42	94.45	1112
1	116.30	81.90	465	1	131.98	97.50	515
2	125.88	86.70	408	2	131.34	100.50	576
3	130.95	91.55	406	3	133.02	103.50	602
4	137.15	96.30	391	4	135.41	106.50	615
5	135.95	101.10	459	5	134.67	109.50	706
6	136.12	105.95	530	6	131.52	112.55	936
7	135.10	110.70	655	7	131.44	115.60	1122
8	128.84	115.50	1198	8	129.40	118.00	1558
9	126.80	118.00	1816	9	129.17	118.00	1590

$$q = 17.77 \times 10^3 \ \text{W/m}^2$$

Run No.8   **Run No.11**

0	116.30	102.77	1313	0	101.57	86.92	1212
1	137.15	105.00	552	1	125.92	90.65	518
2	132.25	107.10	706	2	136.05	94.40	427
3	137.15	109.30	638	3	135.10	98.20	482
4	137.15	111.50	692	4	137.15	102.00	505
5	135.83	113.65	801	5	137.15	105.75	566
6	132.20	115.90	1090	6	133.82	109.50	730
7	131.60	118.00	1306	7	132.30	113.25	932
8	130.03	118.00	1477	8	129.69	117.00	1400
9	130.15	118.00	1462	9	127.90	118.00	1795

Run No.9   **Run No.12**

0	110.98	96.35	1214	0	88.13	70.20	990
1	132.63	99.15	531	1	106.04	75.80	587
2	142.46	102.00	439	2	123.82	81.50	420
3	143.27	104.65	460	3	127.94	87.10	435
4	143.98	107.45	486	4	133.84	92.70	432
5	139.27	110.25	612	5	134.21	98.30	495
6	133.33	113.00	874	6	133.88	103.85	591
7	130.78	115.75	1181	7	132.20	109.50	782
8	128.72	118.00	1657	8	129.50	115.05	1230
9	128.08	118.00	1762	9	127.37	118.00	1896

$z \times 10^{-2}$ mm	Temperature, °C		h W/m²°C	$z \times 10^{-2}$ mm	Temperature, °C		h W/m²°C
	t_W	t_L			t_W	t_L	

$q = 19.55 \times 10^3$ W/m²

Run No.13

0	118.30	101.65	1335	0	101.32	92.65	1435
1	137.15	104.10	592	1	114.17	94.70	639
2	137.15	106.55	639	2	120.30	96.70	527
3	137.65	109.10	685	3	123.03	98.70	512
4	141.22	111.65	661	4	125.10	100.75	511
5	139.09	114.10	782	5	123.53	102.80	600
6	134.45	116.65	1098	6	115.87	104.90	1153
7	133.05	118.00	1300	7	115.23	107.00	1512
8	131.21	118.00	1480	8	114.17	107.00	1735
9	130.05	118.00	1622	9	112.08	107.00	2450

Run No.14 (left), Run No.17 (right)

0	112.05	97.72	1365	0	87.27	80.70	1895
1	136.32	100.50	546	1	103.47	84.00	639
2	146.37	103.15	452	2	111.62	87.25	510
3	144.35	105.90	508	3	114.85	90.50	511
4	146.16	108.50	519	4	117.15	93.80	538
5	143.93	111.20	597	5	116.93	97.10	628
6	136.15	113.90	879	6	122.67	100.50	561
7	133.27	116.60	1173	7	126.10	103.80	558
8	131.00	118.00	1504	8	116.30	107.00	1337
9	129.42	118.00	1711	9	111.62	107.00	2690

43.25 wt % WATER

$q = 12.44 \times 10^3$ W/m2

Run No.15 (left), Run No.18 (right)

0	103.13	95.67	1668	0	84.02	74.20	1266
1	116.70	97.30	641	1	100.31	78.10	560
2	122.61	99.10	529	2	108.00	82.00	478
3	125.96	101.00	498	3	111.38	85.90	488
4	126.38	102.70	526	4	116.30	89.80	469
5	124.84	104.50	612	5	116.50	93.70	546
6	127.83	106.35	579	6	121.15	97.70	531
7	126.77	107.00	629	7	120.51	101.70	661
8	116.50	107.00	1310	8	116.28	105.65	1170
9	113.91	107.00	1800	9	113.30	107.00	1974

$z \times 10^{-2}$ mm	Temperature, °C		h W/m² °C	$z \times 10^{-2}$ mm	Temperature, °C		h W/m² °C
	t_W	t_L			t_W	t_L	

$$q = 14.22 \times 10^3 \text{ W/m}^2 \qquad q = 15.99 \times 10^3 \text{ W/m}^2$$

Run No.19   Run No.22

$z \times 10^{-2}$ mm	t_W	t_L	h	$z \times 10^{-2}$ mm	t_W	t_L	h
0	103.38	97.42	2396	0	104.72	97.55	2230
1	118.28	98.90	733	1	118.73	99.00	810
2	125.60	100.50	567	2	126.18	100.50	623
3	128.61	102.10	536	3	128.86	102.00	595
4	130.53	103.70	530	4	131.46	103.50	572
5	127.37	105.25	643	5	127.20	105.00	720
6	125.95	107.00	750	6	116.81	106.60	1566
7	121.34	107.00	991	7	115.31	107.00	1925
8	117.13	107.00	1404	8	114.58	107.00	2110
9	114.36	107.00	1932	9	113.94	107.00	2305

Run No.20   Run No.23

$z \times 10^{-2}$ mm	t_W	t_L	h	$z \times 10^{-2}$ mm	t_W	t_L	h
0	95.90	87.50	1693	0	92.28	83.16	1755
1	112.05	90.10	648	1	109.80	86.30	680
2	118.40	92.75	554	2	117.97	89.50	562
3	118.30	95.40	621	3	119.80	92.65	589
4	122.17	98.00	588	4	122.53	95.90	600
5	122.65	100.75	649	5	121.70	99.10	707
6	126.83	103.50	610	6	120.10	102.40	903
7	124.55	106.20	775	7	117.60	105.60	1333
8	117.23	107.00	1390	8	115.27	107.00	1934
9	113.69	107.00	2126	9	114.00	107.00	2285

Run No.21   Run No.24

$z \times 10^{-2}$ mm	t_W	t_L	h	$z \times 10^{-2}$ mm	t_W	t_L	h
0	92.57	79.53	1090	0	86.25	76.72	1678
1	105.30	83.00	638	1	105.40	80.55	643
2	113.85	86.65	523	2	114.43	84.50	535
3	117.57	90.20	520	3	116.40	88.50	573
4	119.90	93.75	543	4	120.50	92.40	569
5	119.68	97.50	638	5	119.87	96.40	681
6	123.66	101.00	628	6	123.00	100.40	707
7	122.40	104.50	794	7	122.65	104.40	876
8	116.15	107.00	1554	8	117.15	107.00	1575
9	113.95	107.00	2045	9	114.60	107.00	2105

$z \times 10^{-2}$ mm	Temperature, °C t_W	t_L	h W/m² °C	$z \times 10^{-2}$ mm	Temperature, °C t_W	t_L	h W/m² °C

$q = 17.77 \times 10^3$ W/m²

Run No.25

0	105.85	99.38	2750
1	120.52	100.65	895
2	128.24	102.00	677
3	129.48	103.50	684
4	131.55	104.85	656
5	127.62	106.20	830
6	117.56	107.00	1683
7	116.30	107.00	1912
8	116.08	107.00	1957
9	115.50	107.00	2090

Run No.28

0	88.52	79.35	1940
1	108.21	82.60	694
2	117.35	86.00	567
3	118.02	89.30	619
4	122.40	92.75	600
5	121.15	96.05	708
6	122.40	99.50	776
7	120.30	102.90	1021
8	116.09	106.25	1807
9	113.96	107.00	2550

Run No.26

0	103.25	95.36	2250
1	119.68	97.10	787
2	127.83	99.00	616
3	130.95	100.70	588
4	130.72	102.50	630
5	125.05	104.30	856
6	118.66	106.05	1410
7	117.10	107.08	1760
8	115.87	107.00	2025
9	115.23	107.00	2160

Run No.29

0	74.12	60.56	1311
1	95.25	66.00	608
2	104.98	71.40	530
3	109.77	76.80	539
4	112.26	82.25	592
5	114.17	87.75	673
6	120.33	92.20	656
7	121.56	98.60	775
8	117.40	104.00	1326
9	114.17	107.00	2480

$q = 19.55 \times 10^3$ W/m²

Run No.27

0	94.90	86.68	2133
1	113.73	89.40	730
2	122.40	92.05	585
3	125.13	94.70	584
4	126.98	97.30	599
5	123.43	100.00	758
6	121.21	102.60	955
7	119.05	105.30	1293
8	116.25	107.00	1922
9	115.20	107.00	2170

Run No.30

0	105.82	98.90	2830
1	121.97	100.10	894
2	128.65	101.40	718
3	129.48	102.60	728
4	130.68	103.90	730
5	126.11	105.20	935
6	116.66	106.50	1926
7	114.80	107.00	2508
8	114.80	107.00	2508
9	115.00	107.00	2444

$z \times 10^{-2}$ mm	Temperature, °C		h W/m^2 °C	$z \times 10^{-2}$ mm	Temperature, °C		h W/m^2 °C
	t_W	t_L			t_W	t_L	

$$\underline{62.75 \text{ wt\% } \text{WATER}}$$
$$q = 10.66 \times 10^3 \text{ W/m}^2$$

Run No. 31   **Run No. 34**

$z \times 10^{-2}$ mm	t_W	t_L	h	$z \times 10^{-2}$ mm	t_W	t_L	h
0	100.55	91.38	2132	0	96.52	80.25	1700
1	118.81	93.30	767	1	98.75	83.25	688
2	127.11	95.50	618	2	102.20	86.30	670
3	129.30	97.60	617	3	103.50	89.25	748
4	132.40	99.70	598	4	108.36	92.25	661
5	124.92	101.80	845	5	109.25	95.25	761
6	119.62	104.00	1252	6	112.47	98.30	753
7	116.66	106.10	1850	7	114.35	101.40	786
8	114.96	107.00	2456	8	112.43	103.00	1130
9	114.80	107.00	2510	9	107.02	103.00	2650

Run No. 32   **Run No. 35**

$z \times 10^{-2}$ mm	t_W	t_L	h	$z \times 10^{-2}$ mm	t_W	t_L	h
0	97.85	89.32	2290	0	72.90	65.80	1501
1	116.36	91.60	790	1	86.03	70.45	684
2	126.32	94.00	605	2	91.75	75.10	640
3	129.65	96.50	590	3	96.16	79.60	644
4	133.82	98.90	560	4	100.75	84.40	652
5	129.70	101.25	687	5	103.50	89.00	735
6	120.29	103.75	1182	6	109.13	93.75	693
7	117.97	106.10	1646	7	112.47	98.50	763
8	117.00	107.00	1955	8	112.26	103.00	1151
9	115.73	107.00	2240	9	107.21	103.00	2530

$$q = 12.44 \times 10^3 \quad \text{W/m}^2$$

Run No. 33   **Run No. 36**

$z \times 10^{-2}$ mm	t_W	t_L	h	$z \times 10^{-2}$ mm	t_W	t_L	h
0	95.93	86.10	1990	0	98.15	93.90	2930
1	115.66	88.60	722	1	108.38	95.30	951
2	125.75	91.20	566	2	112.64	96.70	780
3	129.92	93.75	541	3	116.23	98.10	686
4	133.63	96.30	524	4	118.47	99.50	656
5	124.72	98.80	755	5	116.92	100.90	776
6	121.78	101.45	962	6	113.55	102.30	1106
7	119.14	104.00	1291	7	110.50	103.00	1660
8	117.06	106.50	1850	8	110.13	103.00	1745
9	115.75	107.00	2235	9	108.42	103.00	2296

$z \times 10^{-2}$ mm	Temperature, °C		h W/m² °C	$z \times 10^{-2}$ mm	Temperature, °C		h W/m² °C
	t_W	t_L			t_W	t_L	

Run No.37

0	84.70	77.78	1800	0	78.25	71.31	2050
1	98.80	81.00	699	1	93.07	75.25	798
2	104.16	84.30	627	2	99.04	79.10	713
3	104.25	87.50	743	3	100.93	83.00	793
4	109.60	90.75	660	4	106.32	86.90	732
5	110.45	93.55	736	5	107.66	90.80	843
6	114.15	97.25	736	6	110.55	94.70	897
7	115.17	100.50	849	7	112.05	98.60	1056
8	110.13	103.00	1745	8	110.21	102.50	1845
9	107.65	103.00	2675	9	108.15	103.00	2760

Run No.40 (header)

$$q = 14.22 \times 10^3 \ \text{W/m}^2 \qquad q = 15.99 \times 10^3 \ \text{W/m}^2$$

Run No.38

0	100.00	95.20	2960	0	96.78	91.71	3154
1	111.66	96.50	938	1	110.92	93.50	917
2	116.87	97.80	745	2	116.27	95.10	755
3	119.97	99.10	681	3	117.15	96.90	790
4	123.65	100.50	614	4	120.52	97.75	702
5	120.52	102.00	768	5	119.62	100.40	832
6	118.60	103.00	911	6	116.94	102.15	1081
7	112.64	103.00	1475	7	113.75	103.00	1486
8	110.51	103.00	1893	8	112.00	103.00	1776
9	109.65	103.00	2140	9	109.37	103.00	2510

Run No.41 (header)

Run No.39

0	84.90	78.77	2320	0	86.25	78.82	2150
1	99.55	81.90	805	1	101.75	82.00	810
2	105.00	85.00	711	2	107.77	85.00	702
3	106.06	88.10	792	3	108.36	88.10	789
4	110.87	91.20	723	4	112.76	91.20	742
5	110.66	94.35	872	5	113.84	94.30	818
6	115.05	97.50	810	6	116.74	97.40	826
7	117.15	100.60	859	7	117.75	100.50	927
8	113.17	103.00	1397	8	113.48	103.00	1525
9	108.40	103.00	2630	9	109.00	103.00	2665

Run No.42

$z \times 10^{-2}$ mm	Temperature, °C		h W/m² °C	$z \times 10^{-2}$ mm	Temperature, °C		h W/m² °C
	t_W	t_L			t_W	t_L	

$$q = 19.55 \times 10^3 \ W/m^2$$

Run No.43   **Run No.46**

$z \times 10^{-2}$ mm	t_W	t_L	h	$z \times 10^{-2}$ mm	t_W	t_L	h
0	89.36	72.87	2135	0	96.44	89.90	2990
1	98.33	76.65	738	1	112.90	91.70	922
2	104.03	80.45	678	2	118.47	93.60	786
3	105.75	84.10	739	3	121.90	95.40	738
4	111.22	87.80	682	4	123.52	97.25	744
5	112.50	91.60	765	5	121.57	99.10	870
6	114.83	95.40	823	6	123.15	100.90	879
7	118.50	99.20	829	7	118.45	102.70	1241
8	113.39	103.00	1540	8	111.07	103.00	2424
9	109.10	103.00	2620	9	110.55	103.00	2590

$$q = 17.77 \times 10^3 \ W/m^2$$

Run No.44   **Run No.47**

$z \times 10^{-2}$ mm	t_W	t_L	h	$z \times 10^{-2}$ mm	t_W	t_L	h
0	97.82	92.68	2460	0	92.75	85.18	2583
1	112.00	94.35	1006	1	109.50	87.45	887
2	119.20	96.00	766	2	115.65	89.80	858
3	120.88	97.60	763	3	116.30	92.10	808
4	124.25	99.20	710	4	120.52	94.50	751
5	122.15	100.80	832	5	119.67	96.80	819
6	117.30	102.50	1200	6	121.42	99.10	876
7	113.40	103.00	1708	7	116.30	101.50	1320
8	111.90	103.00	1996	8	112.50	103.00	2060
9	110.64	103.00	2330	9	110.68	103.00	2550

Run No.45   **Run No.48**

$z \times 10^{-2}$ mm	t_W	t_L	h	$z \times 10^{-2}$ mm	t_W	t_L	h
0	90.44	83.80	2656	0	90.13	82.18	2460
1	105.64	86.50	929	1	107.57	84.75	856
2	114.15	89.00	707	2	113.45	87.50	753
3	113.75	91.60	802	3	112.85	90.10	860
4	116.30	94.20	804	4	117.08	92.80	805
5	118.60	96.90	819	5	117.77	95.50	878
6	120.52	99.50	845	6	122.00	98.20	821
7	120.72	102.15	958	7	121.80	101.00	940
8	113.32	103.00	1723	8	112.50	103.00	2060
9	112.05	103.00	1964	9	110.38	103.00	2650

$z \times 10^{-2}$ mm	Temperature, °C		h W/m² °C	$z \times 10^{-2}$ mm	Temperature, °C		h W/m² °C
	t_W	t_L			t_W	t_L	

Run No.49

				Run No.52			
0	75.13	66.00	2140	0	86.92	78.65	2580
1	94.20	70.50	825	1	103.35	81.70	985
2	103.05	75.00	697	2	112.37	84.70	771
3	106.06	79.45	735	3	114.58	87.80	796
4	110.72	83.90	728	4	118.49	90.80	770
5	112.68	88.50	809	5	118.70	93.80	856
6	116.50	93.10	835	6	121.24	96.85	875
7	118.95	97.70	920	7	117.51	100.00	1217
8	113.70	102.25	1706	8	111.93	103.00	2390
9	110.43	103.00	2630	9	110.70	103.00	2770

$$q = 21.33 \times 10^3 \ \text{W/m}^2$$

86.50 wt % WATER

$$q = 10.66 \times 10^3 \ \text{W/m}^2$$

Run No.50

				Run No.53			
0	95.82	89.40	3320	0	82.73	78.85	2750
1	111.62	91.50	1060	1	93.07	81.80	946
2	118.77	93.50	844	2	97.43	84.60	831
3	120.42	95.50	855	3	99.08	87.50	921
4	123.88	97.70	815	4	104.14	90.25	767
5	121.03	99.75	1002	5	105.20	93.15	885
6	117.60	101.90	1358	6	109.22	96.00	807
7	113.32	103.00	2067	7	111.22	99.00	872
8	112.00	103.00	2370	8	108.60	100.00	1240
9	110.93	103.00	2690	9	105.00	100.00	2132

Run No.51

				Run No.54			
0	90.22	81.35	2404	0	70.36	61.18	2060
1	108.91	84.00	856	1	82.50	69.60	826
2	116.20	86.75	724	2	87.76	74.05	778
3	116.42	89.50	792	3	91.25	78.50	836
4	120.70	92.25	750	4	98.24	83.00	700
5	120.52	95.00	835	5	100.95	87.50	793
6	121.35	97.70	902	6	105.50	92.00	790
7	117.48	100.50	1255	7	109.75	96.50	805
8	111.66	103.00	2462	8	109.92	100.00	1075
9	110.75	103.00	2750	9	105.00	100.00	2132

$z \times 10^{-2}$ mm	Temperature, °C t_W	t_L	h W/m² °C	$z \times 10^{-2}$ mm	Temperature, °C t_W	t_L	h W/m² °C

$$q = 12.44 \times 10^3 \; W/m^2 \qquad\qquad q = 15.99 \times 10^3 \; W/m^2$$

Run No.55   Run No.58

$z \times 10^{-2}$ mm	t_W	t_L	h	$z \times 10^{-2}$ mm	t_W	t_L	h
0	92.02	87.87	3000	0	99.17	94.87	3720
1	100.90	89.60	1100	1	106.75	95.90	1545
2	105.90	91.50	864	2	111.12	97.00	1133
3	108.70	93.15	800	3	112.20	98.00	1126
4	111.36	95.00	761	4	114.54	99.00	1030
5	111.05	96.70	867	5	111.90	100.00	1344
6	111.19	98.50	980	6	108.08	100.00	1980
7	107.15	100.00	1740	7	106.58	100.00	2430
8	105.67	100.00	2195	8	106.58	100.00	2430
9	105.05	100.00	2466	9	106.54	100.00	2446

Run No.56   Run No.59

$z \times 10^{-2}$ mm	t_W	t_L	h	$z \times 10^{-2}$ mm	t_W	t_L	h
0	73.96	68.55	2300	0	84.18	77.82	2515
1	86.03	72.60	927	1	97.60	80.70	946
2	91.75	76.50	816	2	101.22	83.70	912
3	94.35	80.50	898	3	102.64	86.70	1003
4	101.27	84.50	742	4	108.05	89.70	872
5	102.18	88.50	910	5	108.85	92.60	985
6	106.67	92.50	878	6	112.37	95.55	951
7	109.84	96.50	933	7	112.37	98.50	1153
8	107.70	100.00	1616	8	109.17	100.00	1745
9	105.13	100.00	2425	9	106.15	100.00	2600

$$q = 14.22 \times 10^3 \; W/m^2$$

Run No.57   Run No.60

$z \times 10^{-2}$ mm	t_W	t_L	h	$z \times 10^{-2}$ mm	t_W	t_L	h
0	79.18	73.74	2610	0	69.60	62.93	2400
1	91.95	77.20	964	1	84.55	67.50	938
2	96.97	80.60	864	2	89.87	72.00	895
3	98.30	84.15	1005	3	93.40	76.75	960
4	104.87	87.65	825	4	100.75	81.40	826
5	105.63	91.15	982	5	101.55	86.00	1029
6	108.21	94.65	1050	6	107.18	90.70	970
7	109.43	98.15	1260	7	110.76	95.20	1028
8	106.55	100.00	2170	8	109.86	100.00	1622
9	105.71	100.00	2490	9	105.80	100.00	2760

$z \times 10^{-2}$ mm	Temperature, °C		h W/m² °C		$z \times 10^{-2}$ mm	Temperature, °C		h W/m² °C
	t_W	t_L				t_W	T_L	

$$q = 17.77 \times 10^3 \ W/m^2 \qquad\qquad q = 19.55 \times 10^3 \ W/m^2$$

Run No.61

				Run No.64			
0	93.80	89.56	4190	0	98.08	94.50	5460
1	104.78	91.25	1314	1	108.08	95.55	1561
2	110.02	93.00	1045	2	113.48	96.55	1155
3	112.78	94.55	975	3	113.43	97.85	1255
4	116.23	96.25	890	4	114.58	99.00	1255
5	113.54	97.90	1136	5	111.23	100.00	1742
6	110.47	99.50	1620	6	108.42	100.00	2322
7	107.80	100.00	2280	7	106.50	100.00	3010
8	106.67	100.00	2666	8	106.93	100.00	2822
9	106.63	100.00	2680	9	107.49	100.00	2610

Run No.62

				Run No.65			
0	84.76	79.30	3255	0	88.10	82.78	3673
1	97.65	82.00	1135	1	101.72	85.45	1202
2	104.20	84.80	916	2	106.70	88.00	1045
3	104.83	87.60	1032	3	108.75	90.45	1069
4	110.68	90.40	876	4	113.21	93.00	922
5	110.60	93.00	1010	5	113.32	95.50	1039
6	111.98	95.70	1091	6	113.05	98.00	1300
7	110.91	98.60	1444	7	109.27	100.00	2110
8	107.70	100.00	2310	8	108.42	100.00	2320
9	106.85	100.00	2594	9	107.80	100.00	2506

Run No.63

				Run No.66			
0	77.62	71.78	3045	0	77.10	71.05	3230
1	90.75	75.50	1165	1	92.10	74.45	1108
2	98.60	79.10	911	2	98.90	78.40	953
3	99.76	82.80	1048	3	100.13	82.00	1078
4	107.88	86.50	864	4	107.88	85.65	880
5	107.61	90.15	1018	5	108.33	89.30	1027
6	111.02	93.80	1032	6	112.07	93.00	1025
7	112.26	97.50	1205	7	113.55	96.75	1163
8	107.80	100.00	2280	8	109.06	100.00	2160
9	107.15	100.00	2485	9	107.80	100.00	2506

$z \times 10^{-2}$ mm	Temperature, °C		h W/m² °C	$z \times 10^{-2}$ mm	Temperature, °C		h W/m² °C
	t_W	t_L			t_W	t_L	

$$q = 21.33 \times 10^3 \ \text{W/m}^2$$

Run No.67

0	91.40	85.71	3750				
1	104.74	87.60	1245				
2	111.06	89.60	994				
3	113.63	91.65	970				
4	117.70	93.80	892				
5	116.25	95.80	1043				
6	112.50	98.00	1470				
7	109.73	100.00	2190				
8	108.21	100.00	2600				
9	108.27	100.00	2580				

Run No.69

0	65.55	58.68	3104
1	82.25	63.60	1143
2	91.31	68.50	935
3	93.77	73.50	1052
4	103.02	78.40	865
5	103.87	83.35	1040
6	108.78	88.20	1035
7	112.75	93.15	1088
8	110.25	98.00	1740
9	108.75	100.00	2440

$$q = 24.88 \times 10^3 \ \text{W/m}^2$$

Run No.68

0	87.71	81.62	3500
1	102.12	84.00	1177
2	108.91	86.50	951
3	110.00	88.90	1010
4	114.58	91.40	920
5	114.17	93.80	1047
6	113.66	96.30	1228
7	111.30	98.80	1705
8	108.55	100.00	2494
9	108.17	100.00	2610

Run No.70

0	70.79	62.37	2955
1	88.89	66.90	1131
2	96.78	71.50	985
3	98.72	76.00	1095
4	107.79	80.55	913
5	108.63	85.20	1061
6	113.08	89.80	1070
7	115.17	94.30	1192
8	111.82	99.00	2105
9	110.34	100.00	2407

APPENDIX   C

PHYSICAL PROPERTIES   OF   LIQUIDS

Table C.1   PHYSICAL PROPERTIES OF GLYCERINE

Molecular Formula :
$$\begin{array}{l} CH_2 - OH \\ CH - OH \\ CH_2 - OH \end{array}$$
; Molecular weight = 92.10

1. Density and Viscosity [21]

t °C	ρ g/cm³	μ x10² g/cm.sec.	t °C	ρ g/cm³	μ x 10² g/cm.sec
20	1.2594	1480	110	1.1976	-
30	1.2547	600	120	1.1876	5.2
40	1.2500	330	130	1.1765	-
50	1.2438	180	140	1.1628	1.8
60	1.2376	102	150	1.1468	-
70	1.2315	59	160	1.1261	1.0
80	1.2239	35	180	-	0.45
90	1.2165	21	200	-	0.22
100	1.2077	13	-	-	-

2. Thermal conductivity [21]

t, °C	25	50	75	100	125	150
k, kcal/m.hr.°C	0.240	0.243	0.246	0.248	0.251	0.254

3. Specific heat [22]

t, °C	0	20	50	100
C, $\dfrac{kcal}{kg°C}$	0.54	0.58	0.60	0.67

4. Latent heat of vaporisation

Latent heat of vaporisation of glycerine, over the temperature range used, was estimated by using the following equation [23]

$$\lambda = 284 - 0.2 \, T$$

where T = absolute temperature, °K

Table C 2   PHYSICAL   PROPERTIES OF WATER-GLYCERINE MIXTURES

1. Density, kg/m³ [24]

wt.% Water	Temperature, °C			
	15	20	25	30
0	1264.15	1261.08	1258.02	1254.95
10	1238.10	1235.10	1232.00	1228.90
20	1211.60	1208.50	1205.45	1202.40
30	1184.15	1181.25	1178.40	1175.65
40	1156.50	1153.80	1151.05	1148.30
50	1128.70	1126.30	1123.75	1121.10
60	1101.45	1099.30	1097.10	1094.75
70	1174.55	1072.00	1070.70	1968.55
80	1048.40	1046.90	1045.25	1043.50
90	1023.25	1022.10	1020.70	1019.05
100	999.13	998.23	997.08	995.68

2. Viscosity c.p [25]

wt.% Water	Temperature, °C								
	20	30	40	50	60	70	80	90	100
40	10.80	7.19	5.08	3.76	2.85	2.29	1.84	1.52	1.28
50	6.00	4.21	3.10	2.37	1.86	1.53	1.25	1.05	0.91
60	3.72	2.72	2.07	1.62	1.30	1.09	0.918	0.763	0.668
70	2.50	1.87	1.46	1.16	0.956	0.816	0.690	-	-
80	1.76	1.35	1.07	0.879	0.731	0.635	-	-	-

3. Thermal conductivity, kcal/m.hr.°C [21]

wt.% Water	Temperature, °C					
	0	20	40	60	80	100
0	-	0.243	0.245	0.247	0.250	0.252
20	0.279	0.284	0.289	0.294	0.299	0.304
40	0.323	0.333	0.343	0.353	0.361	-
60	0.373	0.389	0.405	0.420	0.432	-
80	0.427	0.449	0.470	0.489	0.503	-
100	0.486	0.515	0.540	0.561	0.576	0.585

C.1 PROPERTY ESTIMATION METHODS FOR MIXTURES

The mixture properties which are not available in the temperature range used, were obtained by extrapolation wherever possible. In most of the cases, properties have been used beyond the available range of temperatures. Therefore some methods which were tested successfully with the available properties of mixtures, have been devised for property estimation.

1. Density

The density of binary liquid mixtures has been calculated by using the bulk, volume-average properties.

$$\rho_m = \phi_1 . \rho_1 + \phi_2 \rho_2$$

where ϕ_1, ϕ_2 = volume fractions of the components 1 and 2 respectively.

ρ_1, ρ_2 = density of component 1 and 2 respectively.

2. Thermal conductivity

The thermal conductivity of the mixtures was estimated as weighted average of thermal conductivities of the pure components at the temperature of the mixture.

3. Spectific heat

The specific heat of the mixtures was calculated as weighted average of the pure component values at the temperature of the mixture.

4. Latent Heats of vaporisation

The latent heats of vaporisationof liquid mixtures were also calculated by taking weighted average of the pure component properties.

5. Coefficient of thermal expansion

The coefficient of thermal expansion was calculated from the density of the mixture by the following equation [26]

$$\beta = - \frac{1}{\rho_m} \left(\frac{d\rho_m}{dT} \right)_P$$

APPENDIX   D

SAMPLE   CALCULATIONS

D.1   General

D.2   Experimental and Predicted Values of Forced
      convective Heat Transfer Coefficients for water

D.3   Experimental and Predicted values of Natural convec-
      tive Heat Transfer Coefficient for water.

D.4   Experimental and Predicted values of Boiling Heat
      Transfer Coefficient for Water.

D.5   Experimental and Predicted Values of Natural Convective
      Heat Transfer coefficient for Water-Glycerine Mixture

D.6   Experimental and Predicted Values of Boiling Heat
      Transfer Coefficient for Water-Glycerine Mixture.

D.1   GENERAL

a.   <u>Calculation of heat transfer surface</u>

Inside diameter of test sec-tion $= 0.01905$ m

Length of heated section $= 0.94$ m

Heat transfer area $A = \pi \times 0.01905 \times 0.94$

$$= 0.05625 \text{ m}^2$$

b.   <u>Calculation of heat flux</u>

$$q = \frac{Q}{A} = \frac{Q}{0.05625} \quad \text{W/m}^2$$

$$= 17.78 \ Q \quad Q/\text{m}^2$$

where Q is in watts.

c.   <u>Calculation of temperature drop across the wall of the test section</u>

The equation of conductive heat transfer in a cylindrical test surface gives the temperature drop across the wall as below.

$$\Delta t_W = \frac{q \ d_o}{2k} \ \ln \frac{d_o}{d_i}$$

where

d_i = i.d . of tube

d_o = i.d + 2 (wall thickness between inner surface and thermocouple bead).

In Run No. 18   for water at z = 0.40 m, $t_W = 105.64^\circ$C

At this temperature, for copper, k = 325 kcal/m.hr.°C

$$\Delta t_W = \frac{17.77 \times 10^3 \times 0.86 \times 0.02063}{2 \times 325} \ln \frac{0.02063}{0.01905}$$

$$= \underline{0.038 \ °C}$$

D.2 EXPERIMENTAL AND PREDICTED VALUES OF FORCED CONVECTIVE HEAT TRANSFER COEFFICIENT FOR WATER

a. Experimental, h

For a heat flux q = 8.88×10^3 W/m² (Table A.4)

$$\Delta t_{av} = 19.68°C$$

$$\therefore \quad h_{Exptl} = \frac{8.88 \times 10^3}{19.68} = \underline{451} \ W/m^2 \ °C$$

b. Predicted, h

At mean liquid temperature t_L and wall temperature t_W

$k_L = 0.5066$ Kcal/m.hr.°C

$\mu_L = 91.52 \times 10^{-6}$ kg.sec/m²

$\beta_L = 2.55 \times 10^{-4}$ / °C

$\nu_L = 0.8903 \times 10^{-6}$ m²/sec.

$\mu_W = 66.36 \times 10^{-6}$ kg-sec/m².

$\rho_L = 997$ kg/m³

Flow rate = 107.2 kg/hr

$$Re = \frac{19.05 \times 10^{-3} \times 107.2}{2.855 \times 10^{-4} \times 91.52 \times 10^{-6} \times 9.81 \times 3600} = 2210$$

$$Gr = \frac{9.81 \times (19.05 \times 10^{-3})^3 (2.55 \times 10^{-4}) \times 19.68}{(0.8903 \times 10^{-6})^2} = 4.08 \times 10^5$$

According to the equation of Sieder and Tate [15]

$$Nu = 1.86 \left[Re \times Pr \times \frac{d}{z} \right]^{1/3} \left(\frac{\mu_L}{\mu_W} \right)^{0.14}$$

$$= 1.86 \left[2210 \times 6.18 \times \frac{19.05}{900} \right]^{1/3} \left(\frac{91.52}{66.36} \right)^{0.14}$$

$$= 12.85$$

Factor for natural convection effect

$$\chi = 2.25 \left[1 + 0.01 \, (Gr)^{1/3} \right] / \log Re$$

$$= 2.25 \left[1 + 0.01 \, (4.08 \times 10^5)^{1/3} \right] / \log 2210$$

$$= 1.17$$

$$\therefore Nu = 12.85 \times 1.17 = 15.02$$

$$h_{Pred} = \frac{15.02 \times 0.5066}{0.01905 \times 0.86} = 465 \quad W/m^2 \text{-}^\circ C.$$

c. Per cent deviation

$$Deviation = \frac{451 - 465}{465} \times 100 = -3.01 \%$$

D.3   EXPERIMENTAL AND PREDICTED VALUES OF NATURAL CONVECTIVE
      HEAT   TRANSFER COEFFICIENT FOR WATER

Run No. 18

Heat flux,   q $= 17.77 \times 10^3$ W/m^2

Inlet liquid temperature, $t_{L_i} = 78.60\ ^oC$

Saturation temperature , $t_s = 99.00\ ^oC$

Point of onset of saturated boiling , $z_s = 0.815$ m

At z = 0.40 m,

Wall Temperature , $t_W = 105.64\ ^oC$

Liquid Temperature, $t_L = 88.50^oC$

Mean film temperature drop = $\Delta t = 12.63\ ^oC$

a. Experimental h_c

$$h_c = \frac{q}{t_W - t_L} = \frac{17.77 \times 10^3}{(105.64 - 88.50)}$$

$$= \underline{1036}\ \text{W/m}^2\ ^oC$$

b. Predicted h_c by proposed correlation

        The proposed correlation for natural convective heat
transfer in a vertical tube is

$$Nu_c = 3.33 \times 10^{-3}\ (Gr\ Pr)^{0.44}\ (z_s/d)^{0.5}$$

and therefore

$$h_c = \frac{k}{d} \times 3.33 \times 10^{-3}\ (Gr\ Pr)^{0.44}(\ z_s/d)^{0.5}$$

The physical properties in the above equation are

taken at
$$t_{av} = \frac{t_{L_1} + t_s}{2} = \frac{78.60 + 99.0}{2} = 88.8^{\circ}C$$

$$Gr = \frac{gd^3 \beta \Delta t}{\nu^2} = \frac{9.81 \times (1.905 \times 10^{-2})^3 \times 6.862 \times 10^{-4} \times 12.63}{(0.3315 \times 10^{-6})^2}$$

$$= 5.34 \times 10^6$$

$$Pr = 1.986$$

$$h_c = \frac{58.43 \times 10^{-2}}{1.905 \times 10^{-2}} \times 3.33 \times 10^{-3} (5.34 \times 10^6 \times 1.986)^{0.44}$$

$$\times \left(\frac{0.815}{0.01905}\right)^{0.5}$$

$$= 821 \quad kcal/m^2.hr.^{\circ}C$$

$$= \underline{955} \quad W/m^2 \, ^{\circ}C$$

c. **Per cent error** $= \dfrac{955 - 1036}{955} \times 100$

$$= \underline{-8.48}$$

D.4 EXPERIMENTAL AND PREDICTED VALUES OF BOILING HEAT TRANSFER COEFFICIENT FOR WATER

Run No. 18 is selected to demonstrate the calculational procedure.

Heat flux , $q = 17.77 \times 10^3 \, W/m^2$

At $z = 0.90$ m

Wall temperature, $t_W = 107.27^{\circ}C$

Liquid temperature, $t_L = 99.00^{\circ}C$

a. Experimental h_B

$$h_B = \frac{17.77 \times 10^3}{(107.27 - 99.00)} = \underline{2020} \quad W/m^2.^{\circ}C$$

b. Predicted h_B by proposed correlation

$$\frac{h_B}{h_c} = 1.62 \times 10^{-3} \left(\frac{\rho_L}{\rho_V} \frac{c}{\lambda} \frac{d}{z_s} \Delta t_{sub} \right)^{-0.33} \left(\frac{t_L}{t_W} \frac{z}{d} \right)^2$$

All the physical properties in the above correlation are taken at the saturation temperature.

$$\left(\frac{\rho_L}{\rho_V} \cdot \frac{c}{\lambda} \cdot \frac{d}{z_s} \Delta t_{sub} \right)^{-0.33} = \left(\frac{959}{0.585} \times \frac{1.007}{539} \times \frac{0.01905}{0.815} \times 20.4 \right)^{-0.33}$$

$$= 0.8825$$

$$\left(\frac{t_L}{t_W} \frac{z}{d} \right)^2 = \left(\frac{99}{107.27} \times \frac{0.90}{0.01905} \right)^2$$

$$= 1900$$

$$h_B = 955 \times 1.62 \times 10^{-3} \times 0.8825 \times 1900$$

$$= \underline{2590} \quad W/m^2.^{\circ}C.$$

c. Per cent error $= \dfrac{2590 - 2020}{2590} \times 100$

$$= \underline{22}$$

D.5 EXPERIMENTAL AND PREDICTED VALUES OF NATURAL
CONVECTIVE HEAT TRANSFER COEFFICIENT FOR WATER-
GLYCERINE MIXTURE

Run No. 38 is chosen for demonstrating the method
of calculation.

Concentration : 62.75 wt.% water

$q = 14.22 \times 10^3$ W/m^2 , $t_{L_1} = 95.20$ °C

$t_s = 103$ °C

Point of onset of saturated boiling $z_s = 0.575$ m

At $z = 0.30$ m,

Wall temperature, $t_W = 119.97$ °C

Liquid temperature, $t_L = 99.10$°C

Mean film temperature drop, $\Delta t = 21.03$ °C

a. Experimental h_c

$$h = \frac{q}{t_W - t_L} = \frac{14.22 \times 10^3}{119.97 - 99.10} = \underline{681} \text{ W/m}^2 \text{ °C}$$

b. Predicted h_c

$$Nu_c = 3.33 \times 10^{-3} (Gr \ Pr)^{0.44} (z_s/d)^{0.5}$$

All the physical properties of the mixture will be

taken at $t_{av} = \dfrac{t_{L_1} + t_s}{2} = 99.10$°C

$$\rho_L = \frac{\frac{62.75}{959}}{\frac{62.75}{959} + \frac{37.25}{1208.5}} \times 959 + \frac{\frac{37.25}{1208.5}}{\frac{62.75}{959} + \frac{3\ 7.25}{1208.5}} \times 1208.5$$

$$= 1039 \ kg/m^3$$

$$\mu_L = 2.30 \ kg/m\text{-}hr \ , \quad \nu_L = 0.219 \times 10^{-2} \ m^2/hr$$

$$k_L = 0.6275 \times 0.5874 + 0.3725 \times 0.2484$$

$$= 0.4612 \quad Kcal/m. \ hr. \ ^\circ C$$

$$C_L = 0.6275 \times 1.0077 + 0.3725 \times 0.668$$

$$= 0.8815 \ kcal/kg. \ ^\circ C$$

$$\beta = - \frac{1}{1039} (-0.75) = 7.22 \times 10^{-4} \ /^\circ C$$

$$(Gr \ Pr)^{0.44} = \left[\frac{9.81 \times (3600)^2 \times (1.905 \times 10^{-2})^3 \times 7.22 \times 10^{-4} \times 21.03}{(0.219 \times 10^{-2})^2} \right.$$

$$\left. \times \ \frac{0.8815 \times 2.30}{0.4612} \right]^{0.44}$$

$$= 1310$$

$$\left(\frac{z_s}{d}\right)^{0.5} = \left(\frac{0.575}{0.01905}\right)^{0.5} = 5.5$$

$$h_c = \frac{0.4612}{0.01905} \times 3.31 \times 10^{-3} \times 1310 \times 5.5 \times 0.86$$

$$= \underline{672} \ W/m^2 \ {}^oC$$

C. Percent error $= \dfrac{672 - 681}{672} \times 100$

$$= \underline{-1.34}$$

D.6 EXPERIMENTAL AND PREDICTED BOILING HEAT TRANSFER
COEFFICIENTS FOR WATER GLYCERINE MIXTURE

Taking $z = 9.80$ for Run No. 38

$$q = 14.22 \times 10^3 \ W/m^2$$

$$t_W = 110.51 \ {}^oC \ , \quad t_L = 103. \ {}^oC$$

a. Experimental h_B

$$h_B = \frac{14.22 \times 10^3}{110.51 - 103.0} = \underline{1893 \ W/m^2}$$

b. Predicted h_B

$$\frac{h_B}{h_c} = 5.42 \times 10^{-4} \left(\frac{\rho_L}{\rho_v} \cdot \frac{C}{\lambda} \cdot \frac{d}{z_s} \Delta t_{sub} \right)^{0.12} \left(\frac{t_L}{t_W} \cdot \frac{z}{d} \right)^{2.3}$$

The physical properties are taken at saturation temperature
of the mixture.

$$\rho_L = \cfrac{\cfrac{62.75}{956.2}}{\cfrac{62.75}{956.2} + \cfrac{37.25}{1204.5}} \times 956.2 + \cfrac{\cfrac{37.25}{1204.5}}{\cfrac{62.75}{956.2} + \cfrac{37.25}{1204.5}} \times 1204.5$$

$$= 1036 \quad kg/m^3$$

Average molecular weight = 25.6

$$\rho_v = \frac{273}{376} \times \frac{25.6}{22.4} = 0.83 \quad kg/m^3$$

$$c = 0.6275 \times 1.0084 + 0.3725 \times 0.675$$

$$= 0.8835 \quad kcal / kg \,^\circ C.$$

$$\lambda = 0.6275 \times 537.5 + 0.3725 \times 208.8$$

$$= 414.7 \quad kcal/kg.$$

$$\left(\frac{\rho_L}{\rho_v} . \frac{c}{\lambda} . \frac{d}{z_s} . \Delta t_{sub}\right)^{0.12} = \left(\frac{1036}{0.83} + \frac{0.8835}{414.7} + \frac{0.01905}{0.575} \times 7.8\right)^{0.12}$$

$$= 0.956$$

$$\left(\frac{t_L}{t_W} . \frac{z}{d}\right)^{2.3} = \left(\frac{103}{110.51} \times \frac{0.80}{0.01905}\right)^{2.3} = 6100$$

$$h_B = 670 \times 5.42 \times 10^{-4} \times 0.956 \times 6100 = \underline{2123 \ W/m^2 \,^\circ C}$$

c. Per cent error $= \dfrac{2123 - 1893}{2123} \times 100$

$$= \underline{10.8}$$

--

REFERENCES

1. Piret, E.L. and Isbin, H.S., "Natural Circulation
    Evaporation, Two-phase Heat Transfer",Chem.
    Eng. Progr., Vol.50(6), pp 305-311(1954).

2. Guerrieri, S.A. and Talty, R.D., " A Study of Heat
    Transfer to Organic Liquids in Single Tube
    Natural-Circulation, Vertical-Tube Reboilers",
    Chem. Eng. Progr.Symp. Ser. 18, Vol.52, pp.69-
    76 (1956).

3. Dengler, C.E. and Addoms, J.N.,"Heat Transfer Mecha-
    nism for Vaporisation of Water in a Vertical
    Tube", Chem. Eng. Progr. Symp. Ser. 18, Vol.52,
    pp 95-102(1956).

4. Lee, D.C., Dorsey, J.W., Moore, G.Z., and Mayfield,
    F.D., " Design Data for Thermosiphon Reboilers",
    Chem. Eng. Progr., Vol.52(4), pp 169-164(April 1956)

5. Johnson, A.I., "Circulation Rates and Overall Tempe-
    rature Driving Forces in a Vertical Thermosiphon
    Reboiler", Chem.Eng. Progr., Symp. Ser. 18,
    Vol.52, pp 37-46(1956).

6. Ladiev, R.Ya, "Limiting Heat Transfer during Boiling
        in Loops with Natural Circulation", Khim.Prom.Uks.
    ... (Russian), 1966(4),30-4(Russ).

7. Claire, A.G., " A Single-Tube Experimental Evaporator",
        Proc. Quensland Soc. Sugar Cane Tech., 34,
        pp. 263-70(1967).

8. Bergles, A.E., Lopina, R.F., and Fiori, M.P.,
        "Critical Heat Flux and Flow Pattern
        Observations for Low Pressure Water
        Flowing in Tubes", Trans. ASME, Ser.C.,
        Vol. 89 (1), p.69(1967)

9. Beaver, P.R. and Hughmark, G.A., " Heat Transfer
        Coefficients and Circulation Rates for Thermo-
        siphon Reboilers" AICh E. J., Vol.4(5),
        pp. 746-749(Sept. 1968)

10. Shellene, K.R., Sternling, C.V., Church, D.M.,
        and Snyder, N.H., " Experimental Study of
        an Industrial size Vertical Thermosiphon
        Reboiler, Chem. Eng. Progr., Symp. Ser.82,
        Vol. 64, pp 102-113 (1968).

11. Takeda, T., Hayakawa, T., and Fujita, S., "Vapour Holdup and Boiling Heat Transfer Coefficient in Natural Circulation Vertical Tube Evaporator," Heat Transfer Japanese Research 2, pp34-43 (Jan-March 1973).

12. Chexal, V.K. and Bergles, A.E., "Two-Phase Instabilities in a Low Pressure Natural Circulation Loop", AIChE Symp. Ser. 131, Vol.69, p.37(1973).

13. Calus, W.F., Denning, R.K., Montegnacco, A.di, and Gadsdon, J., " Heat Transfer in a Natural circulation Single Tube Reboiler-Part I" The Chemical Engg. Journal, Vol.6(3), pp 233-250 (1973).

14. Calus, W.F., Denning, R.K., and Montegnacco, A.di, "Heat Transfer in a Natural Circulation Single Tube Reboiler- Part II", The Chemical Engg. Journal Vol.6(3), pp.251-264 (1973).

15. Jakob, M., "Heat Transfer-Volume I", John Wiley and Sons, Inc., New York, pp.544-546(1964).

16. Alam, S.S. and Varshney, B.S., "Heat Transfer Studies in Pool Boiling of Subcooled Liquids in a Horizontal Tube" Indian Journal of Tech. Vol.10, pp 172-175 (1972).

17. Alam, S.S., "Nucleate Pool Boiling of Liquid Mixtures" Ph.D. Thesis, University of Roorkee, Roorkee(1972)

18. Lapin, Y.D., Therm. Eng. (USSR), Vol.16(9),pp 94-97(1969)

19. Varshney, B.S. and Stushin, N.G., "Boiling Heat Transfer of Subcooled Liquids in Horizontal Tube-II" Indian Chemical Engineer, Vol.II (April 1969).

20. Moles, F.D. and Shaw, J.F.G., " Boiling Heat Transfer to Subcooled Liquids under conditions of Forced Convection", Trans. Instn. Chem. Engrs, Vol.50(1), p.76(1972).

21. Vargaftic, N.B. "Hand Book on Physical Properties of Gases and Liquids", Gasudarstvenae Isdalelstvo Physico-Mathematicheskoe Literaturee, Moskava (1963)

22. "International Critical Tables", Vol.V, McGraw Hill Book Company Inc. N.Y. (1929).

23. Sternling, C.V. and Tichacek, L.J., "Heat Transfer Coefficient for Boiling Mixtures Experimental Data for Binary Mixtures of Large Relative Volatility.

24. Perry, J.H., "Chemical Engineers' Hand Book", 4th ed., McGraw-Hill Book Company Inc (1963).

25. Newman, A.A., "Glycerol", Morgan-Grampian, London(1968).

26. Kays, W.M.," Convective Heat and Mass Transfer" McGraw-Hill Book Company Inc. New York, p. 52 (1966).

--